Energy Geoscience 1 (2020) 174–193

Contents lists available at ScienceDirect

Energy Geoscience

journal homepage: www.keaipublishing.com/en/journals/energy-geoscience

Review

The Pliocene-Recent Euphrates river system: Sediment facies and architecture as an analogue for subsurface reservoirs

Dorrik Stow [a, *], Uisdean Nicholson [b], Samantha Kearsey [b], Dominic Tatum [a], Andy Gardiner [a], Amer Ghabra [c, 1], Mahmoud Jaweesh [d, 2]

[a] EGIS-IGE, Heriot-Watt University, Edinburgh, EH14 4AS, UK
[b] Glasgow International College, 56 Dumbarton Road, Glasgow, G11 6NU, UK
[c] Department of Geology and Petroleum Exploration Engineering, Faculty of Petroleum Engineering, Syrian Private University, Damascus, Syria
[d] School of Geography, University of Birmingham, Birmingham, B15 2TT, UK

ARTICLE INFO

Article history:
Received 4 May 2020
Received in revised form
16 July 2020
Accepted 20 July 2020

Keywords:
Euphrates river
Fluvial facies
Fluvial architecture
Reservoir analogue

ABSTRACT

The Tigris-Euphrates is a continental-scale fluvial system, around 2800 km in length, which drains over 1 million km^2 of SW Asia. The system originated in the Late Miocene and developed into the principal axial drainage system of the region, which follows broad regional structural features of the Mesopotamian Foreland Basin. Good preservation and outcropping of the Pliocene and Quaternary Euphrates deposits yield a viable local analogue for subsurface fluvial reservoirs in the region, and for other fluvial systems that have developed in foreland basin settings. This paper documents the first detailed study of the sedimentary characteristics of these Pliocene and Quaternary fluvial deposits along the middle reaches of the present-day Euphrates in Syria.

The Euphrates fluvial system developed from small and probably short-lived isolated cut-and-fill channels in the Pliocene, characterised by abundant debrite and slump facies, through to a broad meandering system at present. The Quaternary deposits represent a braided to meandering system that was more energetic than that of the modern day Euphrates. The Quaternary facies include a dominance of gravels, pebbly sands and sands as channel associations, coupled with sands, muds and paleosols representing channel abandonment, overbank and crevasse-splay associations. Channel widths, where observed, range from 50 to 500 m, and minimum fill thicknesses range from 3 to 7 m. The combined channel-fill for stacked channels is up to 25 m thick. Lateral correlation of channel elements over at least 1 km of section indicates that rapid and extensive lateral migration has occurred. Crevasse splay lobes can be identified in the overbank deposits, with a width of 30–60 m and sand thickness of 0.5–1.5 m. The geometry, nature and dimensions of these architectural elements provide a useful analogue for subsurface reservoirs. The high-energy channel facies of the Quaternary system show very good reservoir attributes, with good correlation and connectivity. At the bed-scale there is significant heterogeneity of characteristics that would impact fluid-flow for hydrocarbon production from a subsurface reservoir. However, incomplete preservation of these Quaternary fluvial deposits at outcrop remains a challenge for accurately determining the scale of sedimentary features and also the size of the paleo-river.

1. Introduction

1.1. Rationale

Rivers, modern and ancient, are a hugely important component of the Earth environment, and their better understanding is key to addressing the Sustainable Development Goals set by the United Nations. Whereas hydrologists, hydrogeologists and civil engineers

* Corresponding author.
E-mail address: d.stow@hw.ac.uk (D. Stow).
[1] now Al-Almarah College University, Iraq.
[2] now Affinity Water, Birmingham, UK.

Production and Hosting by Elsevier on behalf of KeAi

https://doi.org/10.1016/j.engeos.2020.07.005

work at very short timescales in seeking to tackle global issues of water resources, reservoirs, aquifers and flood hazards, geoscientists focus on the very long timescales of river basin evolution and the preservation of their deposits in the geological record. Their work contributes to the evaluation and use of subsurface aquifers for water supply, subsurface reservoirs for oil and gas resources, and both aquifers and reservoirs for carbon dioxide sequestration in mitigation of global warming. Combining the study of modern day river processes with ancient fluvial analogues gives a greater awareness of the impact of longer term boundary conditions playing on the modelling and prediction of fluvial systems and their role in the storage of important resources (Miall, 2006, 2010; Corbett et al., 2019).

The broad significance of geological studies of fluvial systems for the better understanding subsurface energy resources has been well documented over the past few decades (Ashton, 1993; Corbett et al., 2019). The specific issues of high-energy braided fluvial systems were considered in detail by Best and Bristow (1993), whereas the low-energy flood plain was expounded by Marriot and Alexander (1999), and the importance of downstream deltaic systems for coal, oil and gas resources has been synthesised in the volume by Whately and Pickering (1989).

Many of the world's hydrocarbon reservoirs are found in fluvial systems, from Precambrian to Pleistocene in age (Miall, 2006; Corbett et al., 2019). Some giant fields include the Clair Field, NW UK continental margin, with alluvial fan to braided fluvial reservoir intervals of both Devonian and Permo-Triassic age; the Prudhoe Bay Field, N Alaskan slope, with braided river reservoir intervals in the Triassic; the Little Creek Field, Mississippi, with meandering river/flood plain reservoir intervals in the mid-Cretaceous; and the Brent cluster of fields in the North Sea, with fluvio-deltaic reservoirs in the mid-Jurassic. What these and many other fluvial fields clearly demonstrate is the complexity of the fluvial reservoir architecture, and its impact on reservoir compartmentalisation (Jolley et al., 2010), on sandbody geometry and heterogeneity (Martinius et al. 2014). It is this complexity that drives the need to study outcrop, subsurface and modern day analogues in order to predict basin-scale alluvial architecture (Yeste et al., 2019), and the efforts to develop machine learning techniques to reveal sedimentological patterns in river deposits (Demyanov et al., 2019). It has also driven part of the rationale behind this paper.

In addition to the obvious economic interest, current research in fluvial sedimentology is concerned, amongst other aspects, with: (a) the link between processes, bedforms and deposits (Best and Fielding, 2019); (b) sediment routing and sediment budgets, including carbon budgets, from source to sink (Nicholson et al., 2014, 2016; Blum, 2019); (c) basin to continent-scale evolution of river systems and their controls (Nicholson et al., 2019); (d) quantification and morphometric analysis of distributive fluvial systems (Weissmann et al., 2010; Owen et al., 2015); (e) modelling, simulation and machine-learning applied to fluvial systems (Martinius et al., 2014; Demyanov et al., 2019); and, perhaps most importantly, the management and evolution of river systems in response to human and climate drivers (Adeloye and Sundharajan, 2019). Our work contributes, in part, to research topics (b) and (c) above, especially in the context of continent-scale drainage system evolution driven by tectonic and sea-level controls.

1.2. Study area and aims

The Tigris-Euphrates river system is the most important drainage basin in SW Asia, covering an area of around 1,050,000 km^2 (Hovius et al., 1998). The Euphrates is approximately 2800 km in length, rising from a source near Mount Ararat in NE Turkey, draining the Taurus Mountains and then flowing generally SE through Syria and Iraq (Fig. 1). It joins the Tigris near Al Quanah in Iraq, where the two become the Shatt El Arab River flowing into the Persian Gulf. The Tigris-Euphrates system developed in the Late Miocene and has since acted as the principal axial drainage route within the foreland basin (Mesopotamian Basin) that has formed as a result of flexure of the Arabian Plate as an isostatic adjustment to the growth of the Zagros Mountains in the north east. It has been classified as "Eurotype" continental drainage system by Dickinson (1988), which is strongly controlled by large-scale structural geomorphology. The system is therefore in a unique tectonic setting relative to most of the Earth's largest continental-scale drainage systems (Nicholson et al., 2014).

The modern Euphrates River has been radically affected by water management activities, which began with early irrigation systems over 5000 years ago and have culminated in the construction of a series of major dams along its upper and middle reaches. Global warming over the past 200 years has had further impact on the drainage basin as a whole, causing it to become more arid and with less discharge.

This study was initiated by Shell Syria, Shell Development Oman and Petroleum Development Oman with the aim of obtaining a database of sandbody geometries and stacking patterns for use as a possible analogue for subsurface reservoirs in the Permo-Triassic Mulussa and Gharif formations in east central Syria. These formations developed in one of the foreland basins associated with uplift of the eastern arm of the Central Pangean Mountains, so their tectonic setting may have been broadly similar to that of the Tigris-Euphrates system. In addition, the architectural data gathered could be used in generic reservoir modelling of fluvial systems.

The fieldwork focuses on well-exposed Pliocene and Quaternary fluvial deposits of the ancestral Euphrates, which outcrop adjacent to the middle reaches of the modern river system between Al Raqqa and Al Bukemal in eastern Syria (Fig. 1). Based on extensive sedimentary mapping and logging, we characterise the principal sedimentary facies and fluvial architecture, and document these for the first time. The data provide an outcrop analogue of fluvial systems in the subsurface that may be of interest for both water resources and/or hydrocarbons. We further consider the sedimentary evolution observed in the context of tectonic development and foreland basin drainage in the region.

2. Methods

Reconnaissance of the main geological features in the middle reaches of the present-day Euphrates was undertaken in two stages: (1) using aerial photography to identify possible outcrops, and (2) ground-truthing in the field to refine the locations of outcrops identified during stage 1. Identifying the main geomorphological features of the modern Euphrates river system was undertaken using Google Earth. The fieldwork was undertaken in January–February 2009, by members of staff from the Institute of Petroleum Engineering at Heriot-Watt University (UK), the University of Damascus (Syria), Al Farat Petroleum Company (AFPC) and the Syrian Petroleum Company (SPC).

In the reconnaissance survey, over 60 different locations were examined between Aleppo and the Syria/Iraq border. Of these, six of the best exposed localities were selected for detailed study (Fig. 2): A - Al Rabbah; B - Ain Ali; C - El Ward and D - Dweir, which are representative of the Upper Pliocene succession; and E – Ayash and F - Al Khawr, which are representative of the Quaternary succession. The present-day Euphrates was observed along the full length of the field study area. Logging of sedimentary sequences was undertaken in the field at a scale of 1:100 for the overall succession in order to describe the vertical variation in sedimentary characteristics of the studied sections. Lateral examination of the

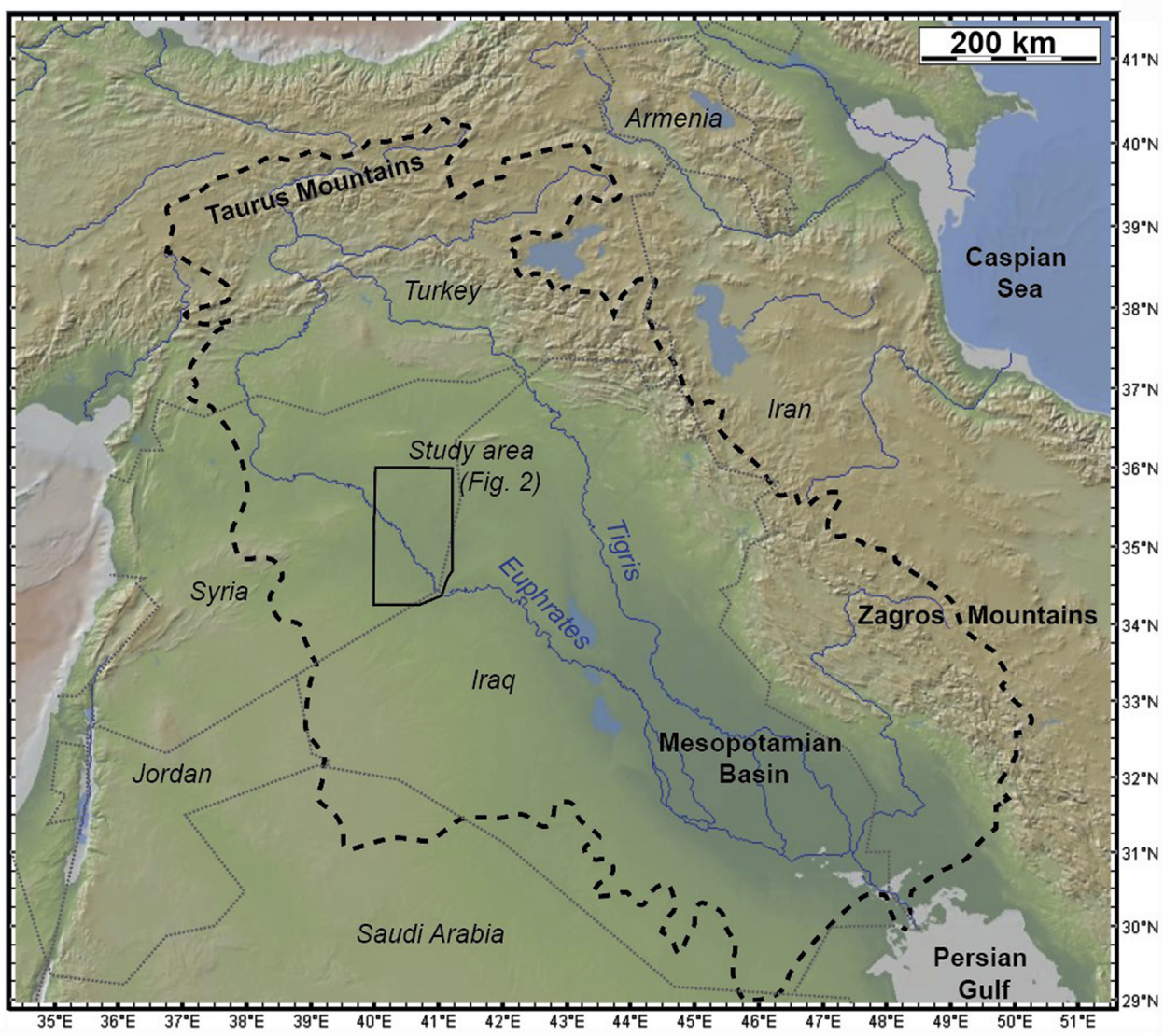

Fig. 1. Location map of the Euphrates-Tigris river system. Black box shows the location of this detailed study of the middle reaches of the Euphrates River in Syria. Country names shown in italics. Geographic names referred to in the text shown in bold. Country outlines shown by grey dashed lines, Tigris-Euphrates drainage basin outlines shown by thick black dashed lines. Background DEM is from GMRT database. Figure is made with GeoMapApp.

exposures was conducted through field observation and measurement, and photo-mosaic annotation.

Detailed logging at a scale of 1:10 was then used for examination of sedimentary structures, textural attributes and compositional characteristics, and as the primary basis for the facies classification scheme developed. This scheme differs slightly from the standard nomenclature (and acronyms) used for fluvial sediments (Miall, 1985, 1996, 2010), in part because we have grouped together some of the facies, and in part because we recognise facies that do not appear in the standard scheme. Interpretation of architectural elements is based on the recognition of facies associations, vertical sequences of facies, and measurement of extensive outcrops that showed lateral relationships.

3. Tectonic and palaeogeographic setting

The Euphrates River has developed within a large foreland basin, the Mesopotamian Basin, which formed as a result of the Late Eocene/Oligocene-Recent collision (Jolivet and Facenna, 2000; McQuarrie and Van Hinsbergen, 2013) between the Arabian and Anatolian Plate in the south and the Eurasian Plate in the north (Fig. 3). During the earliest stage of collision in the latest Eocene, Arabia was part of the African Plate. The ~35-27 Ma collision was characterised by compressional deformation coeval with sedimentation and the formation of significant regional unconformities in the Zagros fold belt (Hessami et al., 2001; Agard et al., 2005). Deformed flysch deposits characteristic of collision and uplift are now exposed close to the suture (Beydoun et al., 1992). Late Oligocene-Early Miocene extension in the SW (Richardson and Arthur, 1988) separated the African and Arabian plates along the Red Sea Rift and accelerated the collision rate of the Arabian Plate to the NE. This event was accommodated on the western margin of the Arabian Plate by the Dead Sea Transform, which is transtensional in the south (Gulf of Aqaba) and transpressional in the north, and led to a major restraining bend with the formation of a long-lived topographic high in Lebanon and SE Syria. This transform boundary formed between 21 and 18.5 Ma in the south and 17.1–12.7 Ma in the north, at the restraining bend. Associated with this is a SW to NE trending series of faults and folds extending to the Palmyrides of Syria, as far inland as the Euphrates River, at the

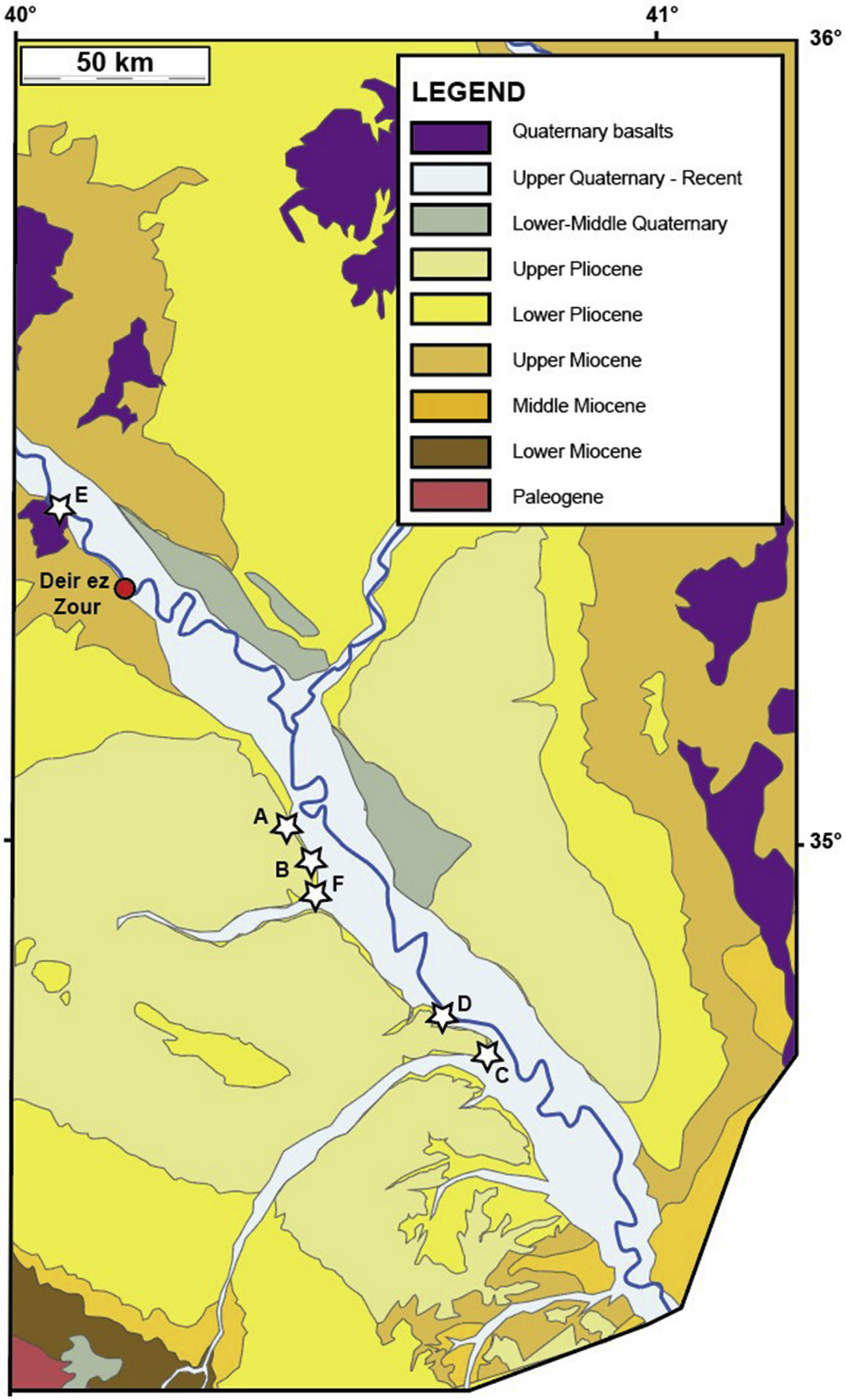

Fig. 2. Simplified geological map of the study area showing the six locations for detailed study as reported in this paper. (A) Al Rabah, (B) Ain Ali, (C) El Ward, (D) Dweir, (E) Ayash Quarry, and (F) Al Khawr Quarry. Note that the Miocene outcrops are not readily visible at this scale because they occur in cliff sections immediately below the Pliocene outcrop at the margins of the modern Euphrates flood plain.

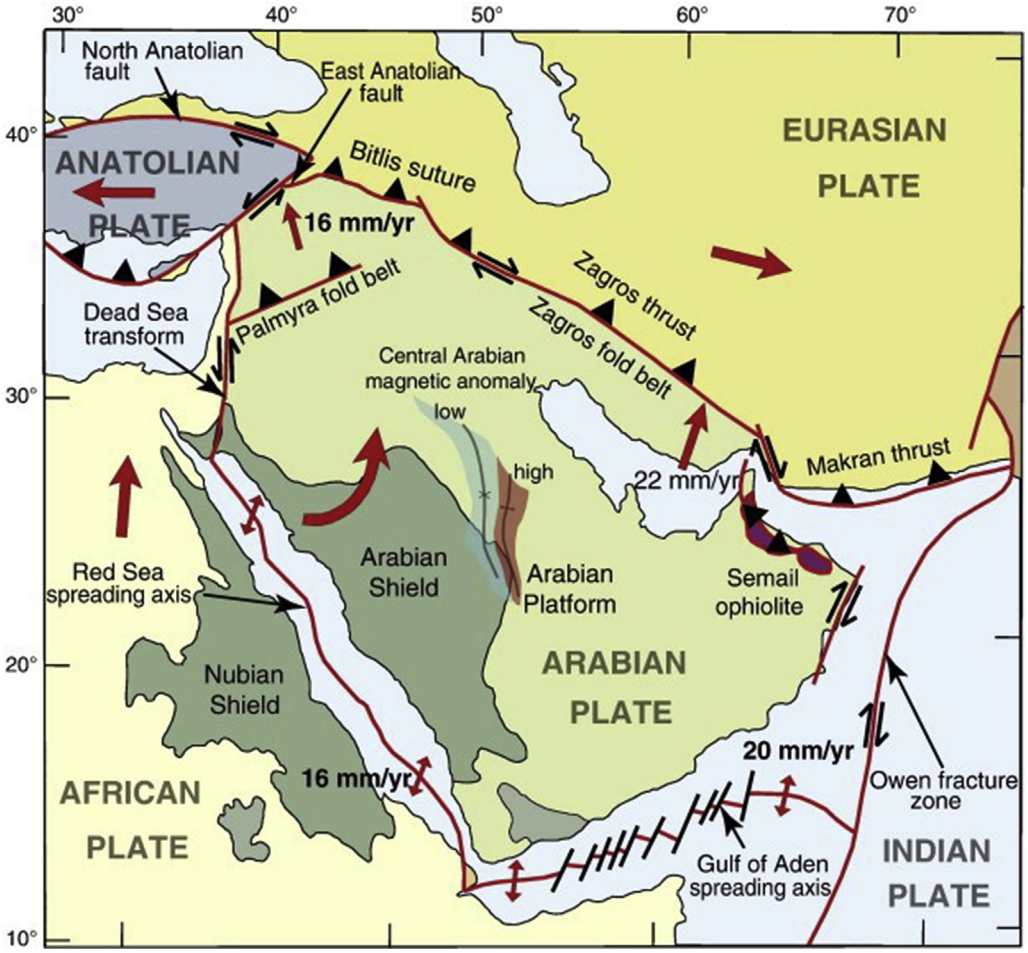

Fig. 3. Regional geological-tectonic setting, with present-day plate boundaries and direction of movement indicated.

northern edge of our field area (Figs. 2 and 3).

During this period (late Oligocene to early Miocene), there was still a continuous seaway between the eastern Mediterranean and the Arabian Sea along the northern edge of the Arabian Plate, where lithospheric flexure caused by the isostatic load of the Taurus-Zagros mountain belt forming along the collision zone resulted in pronounced subsidence of the underthrust plate. Ongoing collision and accommodation of far-field stresses by different structural elements through the Early and Middle Miocene resulted in episodic opening and closure of shallow marine seaways between the Arabian Sea, eastern Mediterranean and Paratethyan basins to the north (Rogl, 1999), which precluded any large drainage systems forming.

However, an increase in sediment supply from the growing Taurus-Zagros orogen to the north began to rapidly fill the foreland basin region from the Early to Middle Miocene onwards, finally separating the different basins in the Serravalian (Rogl, 1999) around 14-12 Ma. A period of reverse faulting and pronounced surface uplift started in the Pliocene, both in the Taurus Mountains to the north (Jaffey and Robertson, 2005) and the Zagros Mountains to the northeast (Leturmy and Robin, 2010). This process of orogenesis and associated erosion, accompanied by drainage integration, resulted in the Mesopotamian foreland basin being rapidly filled by clastic detritus. Collision and surface uplift in the Zagros region was diachronous, propagating from NW to SE, and the stratigraphic evolution of the foreland basin is closely connected to this deformation, with the Mesopotamian foredeep migrating to the south and east through time. The underfilled foreland basin in the present day is represented by the Persian Gulf, where the Shatt Al-Arab delta is situated.

4. Stratigraphy

A detailed discussion of the stratigraphy of SE Syria, where our work is focussed, is beyond the scope of this study, but a brief review of the Neogene and Quaternary succession is relevant. The review of the stratigraphy presented here is based on a synthesis of data from a range of publications (as below) and company reports. It is also shown on Russian geological maps of the area produced by V.O Technoexport under the guidance of the Syrian Ministry of Industry in the 1960 (Fig. 2). Although there is some regional variation in the detailed stratigraphic terminology (e.g. formation names), there is agreement on the broad stratigraphy. This is what we have used in our study and is shown in Table 1.

4.1. Miocene & Pliocene

The Lower Miocene consists mainly of limestone with subordinate shales (Euphrates Formation), which are overlain by limestone (Jaribe Formation), and gypsum with marls (Lower Fars Formation). There is either an unconformity or a transition zone (Doura Europos Formation) between the mainly gypsiferous sediments and the overlying Upper Pliocene pebbly sandstones, sandstones and mudstones (Mayadin Formation). The geological maps of the

Table 1
The stratigraphy of the Neogene and Quaternary systems of Syria, as applied in this study.

Period	Series	Stage	Group/Formation	Lithology
Quaternary			Al Furat Group	Sands and gravels
Neogene	Pliocene	Upper	Mayadin Formation	Sands, gravels and muds
		Lower	Doura Europos formation	Gypsum, fine clastics and rare limestone
	Miocene	Upper	Lower Fars formation	Gypsum and marls
		Middle	Jaribe formation	Limestone
		Lower	Euphrates limestone	Limestones with subordinate shales

Euphrates Valley of SE Syria show that the transition from fine-grained, gypsiferous sediments to coarser clastics without gypsum occurs earlier in the north of the field area (around Al Raqqa) than in south, around Abou Kamal (see Fig. 2 for locations). Pliocene-age deposits of gypsum are locally present in the south. The Pliocene clastics are overlain unconformably by Quaternary sands and gravels of the Al Furat Formation.

4.2. Quaternary

The Quaternary geology, geomorphology and archaeology of the Euphrates river valley were first documented in the early 1960s. Further systematic studies were then carried out on the late Cenozoic deposits and the geomorphology of the river valley when geological mapping of Syria was undertaken (Ponikarov, 1966; Ponikarov et al., 1967). The Pliocene series was divided into two units Na2 and Nb2, and the Quaternary sediments were divided into four river terraces, plus recent floodplain and channel deposits. Although the Quaternary terraces were assigned as belonging either to the Early, Middle or Late Pleistocene or Early Holocene by Ponikarov et al. (1967), the stratigraphic division has since changed. Further research by Besancon and Sanlaville (1981) led to five principal river terraces being identified along the modern Euphrates river, not including the present-day channel and floodplain deposits. Pleistocene volcanic activity has locally intruded the Quaternary succession (Fig. 2) and flowed across some of the terraces. The terrace stratigraphy has therefore been improved by Sharkov et al. (1998), Demir et al. (2007) and Trifonov et al. (2013) who all applied K-Ar dating to basalts overlying terrace deposits in the Euphrates valley. The currently accepted stratigraphy for the Euphrates terraces is given in Table 2. However, without access to dating, our study does not differentiate between these subdivisions of the Quaternary, and we simply group them as the Al Furat Formation.

5. Results

5.1. Sediment facies

Both the Quaternary and Upper Pliocene successions show a similar assemblage of facies, and so they are discussed together in the following section. Sixteen distinct facies are recognised, which can be loosely grouped as: (A) Gravels, (B) Sands, (C) Fine-grained sediments, (D) Chaotica, (E) Paleosols, and (F) Limestones.

These facies are distinguished on the basis of bedding, sedimentary structures, and grain size characteristics, as described in the following paragraphs, and illustrated in Fig. 4. Table 3 summarises their principal characteristics and likely process interpretation, and keys our facies and codes into those of other fluvial systems as standardised by Miall (1996, 2010). We use the standard terminology for bed thickness (Stow, 2005): very thick = >1 m, thick = 0.3–1 m, medium = 0.1–0.3 m, thin = 0.03–0.1 m, very thin = 0.01–0.03 m. A lamina is taken as <0.01 m. As an indication of the overall average occurrence of the different facies, as measured through the logged and sketched sections, we use the following scheme: rare <1%, minor 1–10%, common 10–20%, and very common >20%.

Compositional attributes were identified only in the field and under hand lens inspection. In general, the sands are quartz rich with a variable lithic component. Lignite fragments are rare, whereas bioclastic clasts (e.g. shell debris) are absent. The pebbles are quartz dominated, with some meta-quartzites and other metamorphic rock types evident (gneissose fabrics). Larger clasts of pinkish and cream-coloured micrites and marlstones are also evident locally. Mostly, the sediments are unconsolidated to poorly consolidated, uncemented to weakly cemented. Only the calcrete facies and micrites/marlstones show pervasive calcite cementation. In some localities, the clasts are coated with a hardened bituminous material.

Reservoir characteristics of the different facies groups can be inferred from their specific sedimentary attributes (especially textural properties as detailed below). However, these data are estimated from field observation, rather than via subsequent laboratory measurement of porosity and permeability. For the most part, they apply to poorly consolidated and unconsolidated sediments, without significant cementation or compaction.

Facies groups A and B are reservoir-prone. Facies Group A (gravels) have high porosity (40–50%) and generally high permeability (1-2 Darcies), although the moderate to very poor sorting decreases this value for some units. The structureless gravels have approximately equivalent kh and kv values, whereas most of the facies have kh » kv. Facies Group B (sands) have moderate to high

Table 2
Stratigraphy of the Euphrates Valley River terraces (after Trifonov et al., 2013).

Terrace	Height above present flood plain (m)	Maximum thickness of alluvium (m)	Inferred age
Q_3-$_4$0	0-5	5	Late Pleistocene and Holocene Present channel and flood plain
Q_2I	7-15	11	Middle Pleistocene (Ionian) Older than 0.4 Ma
Q_1II	15-25	14	Late Early Pleistocene (Calabrian) Older than 0.7 Ma
Q_1II[a]	30-45	5	Early Pleistocene Circa 1.2–1.8 Ma (Early Calabrian)
q_1III[b]	45-60	18	Early Pleistocene (Gelasian) Older than 2.12 Ma
N_{22}IV	80-100	>20	Late Pliocene (Piacenzian) Older than 2.8 Ma

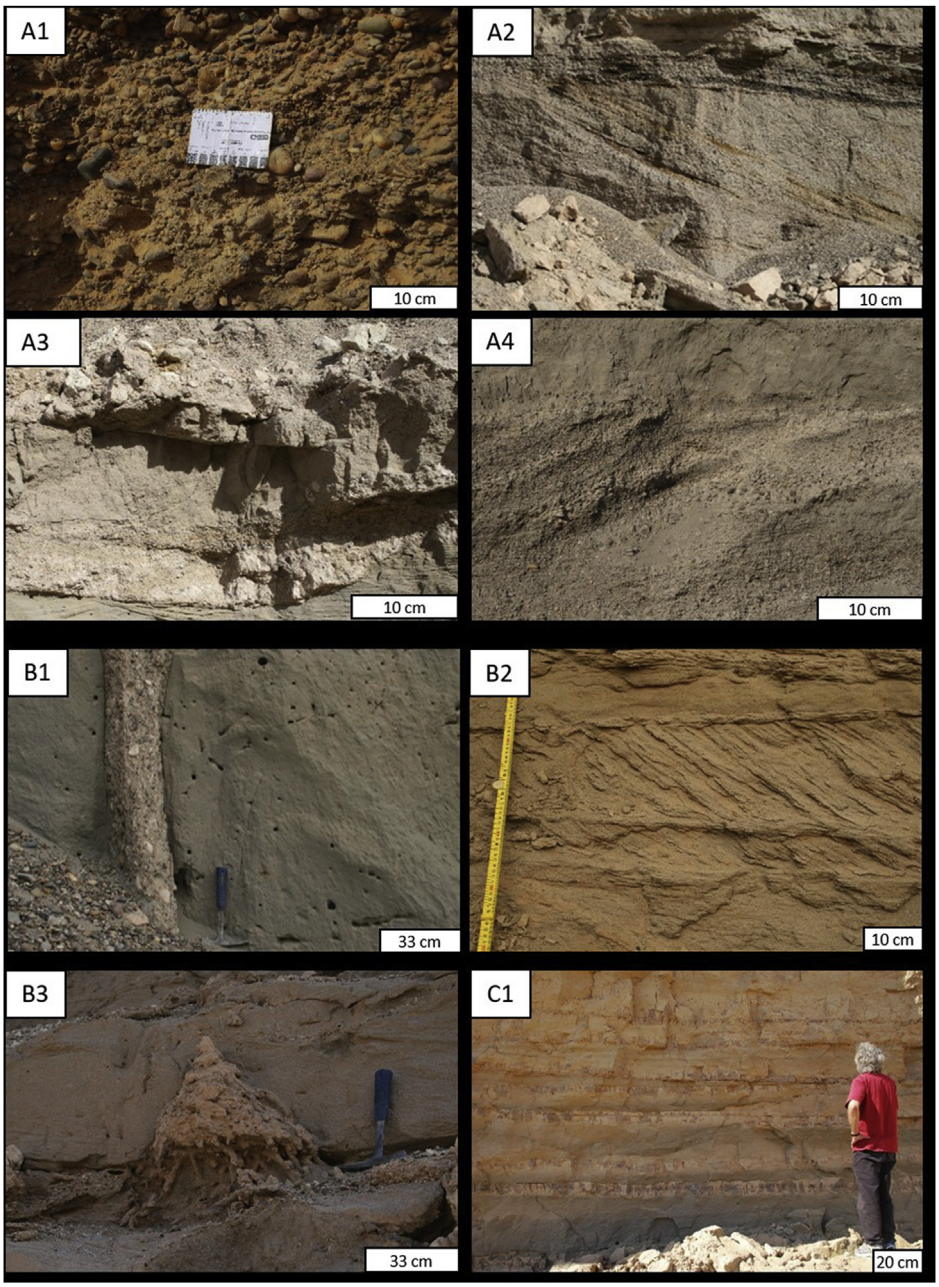

Fig. 4. Photographs of the 16 facies types identified in the Euphrates Pliocene-Quaternary fluvial system. Codes on the photos correspond to the facies codes in the text.
Facies A1: Structureless gravels (Rare occurrence).
Facies A2: Laminated gravels (Common occurrence).
Facies A3: Structureless pebbly sands/sandy gravels (Minor occurrence)
Facies A4: Laminated pebbly sands/sandy gravels (Very common occurrence)
Facies B1: Structureless sands (Common occurrence).
Facies B2: Laminated sands (Very common occurrence).
Facies B3: Bioturbated sands and muddy sands (Common occurrence).
Facies C1: Silts (Minor occurrence).
Facies C2: Muds (Rare occurrence).
Facies D1: Chaotic clast-rich sands and gravels (Minor occurrence).
Facies D2: Chaotic/disturbed sand unit (Rare occurrence).
Facies D3: Chaotic/disturbed pebbly sands and gravels (Rare occurrence).
Facies D4: Slump-folded/disturbed sand/mud units (Rare occurrence).
Facies E1: Calcrete surface (Very common occurrence).
Facies E2: Paleosol horizons and paleo-calcrete surfaces (Rare occurrence).
Facies F: Micrite, muddy micrite, marlstone (Rare occurrence).

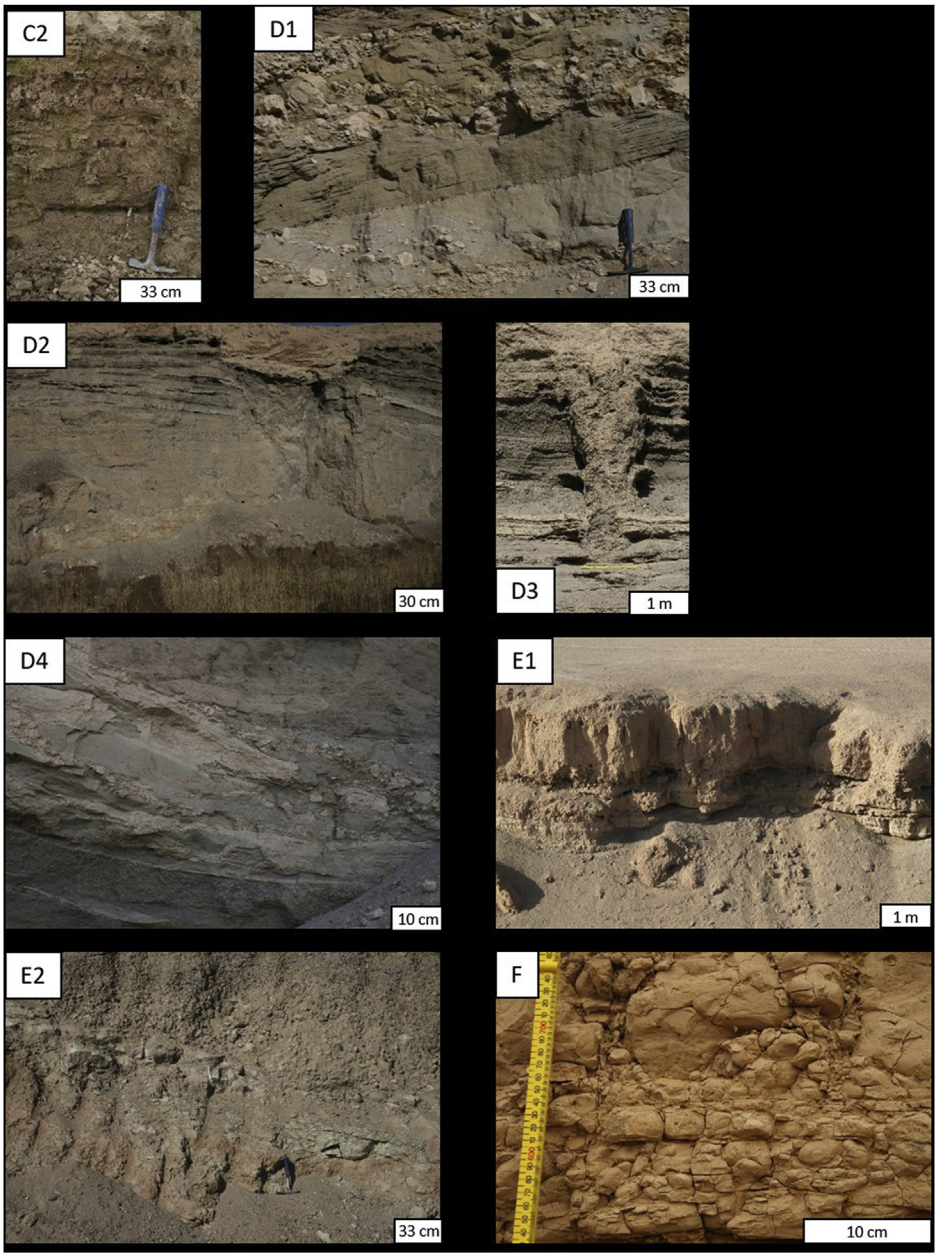

Fig. 4. (*continued*).

porosity (25–45%) and moderate to high permeability (0.5–3 Darcies). The structureless sands show the best kv and kh values, the laminated sands have kh » kv, and the bioturbated/muddy sands show generally lower values.

Facies groups C, E and F are reservoir-poor. Facies Group C (silts and muds) shows a wide range of porosity values (10–25%), but generally low to very low permeability (10-100 mD). Facies Group E and F (calcretes, paleosols, micrites) have reduced values for both porosity and permeability dependent on the amount of carbonate cementation. It is not possible to give reliable estimates for these facies.

Facies Group D is very varied. The injectionite sands and gravels have generally high porosity and permeability (as for facies groups A and B) cross-cutting the bedding. The chaotic and disturbed facies vary according to their dominant grain size.

5.2. Facies characteristics

Facies A1: Structureless gravels (Rare occurrence) (Fig. 4A).

Bedding/structure: Generally thick-to very thick-bedded units with irregular to wedge-shaped bedding, sharp to gradational tops, sharp and erosive to gradational bases. Chaotic internal organisation and clast/grain fabric, generally with no apparent sedimentary structures, although indistinct oscillation grading is evident in some cases.

Texture: Very variable grain size characteristics, poor to very poor sorting, pebbles typically 4–32 mm, sub-rounded to sub-angular, with large angular to rounded clasts up to 600 mm in places.

Interpretation: High energy, rapid deposition, locally erosive; lag deposits, longitudinal bars, rapid channel-fill (flood events), granular debris flow.

Table 3
Summary of principal characteristics and likely process interpretations of the sixteen distinct facies recognized in the Quaternary and Upper Pliocene successions of the Euphrates in Syria.

FACIES CODE this study	FACIES CODE modified from Miall (2010)*	FACIES DESCRIPTIVE NAME	PROCESS/BEDFORM INTERPRETATION
A1	Gm	Structureless gravels	High energy, rapid deposition, locally erosive; lag deposits, longitudinal bars, rapid channel-fill
A2	Gt, Gp, Gh	Horizontal and cross-bedded gravels	High energy, deposition via traction, unidirectional flow, locally erosive; transverse/longitudinal bedforms
A3	GSm, SGm	Structureless sandy gravels and pebbly sands	High energy, rapid deposition, locally erosive; longitudinal bars, rapid channel-fill
A4	GSt, GSp, GSh, SGt, SGp, SGh	Horizontal and cross-bedded sandy gravels and pebbly sands	High energy, deposition via traction, unidirectional flow, locally erosive; transverse/longitudinal bedforms
B1	Sm	Structureless sands	Moderate-high energy, rapid deposition, locally erosive; channel-flood deposits
B2	St, Sp, Sr, Sh	Horizontal and cross-bedded sands	Moderate-high energy, deposition via traction, unidirectional flow; transverse/longitudinal bedforms
B3	Sb, SFb*	Bioturbated sands and muddy sands	Rootlet bioturbation of fluvial sediments during periods of local non-deposition
C1	Fm, Fr, Fh, Fb*	Structureless, laminated and bioturbated silts	Low energy, deposition from suspension/traction, unidirectional flow where cross lamination is apparent
C2	Fm, Fh, Fb*	Structureless, laminated and bioturbated muds	Low energy, deposition from suspension, tranquil setting, and/or traction where lamination present
D1	Gc, Sc*	Chaotic clast-rich sands and gravels	High energy, deposition from debris flows
D2	Sc*, Sd*	Disturbed sands with chaotic or contorted lamination	Disturbance of unconsolidated wet sediment caused by seismic tremor or sudden debris flow/flood event
D3	Gi*, SGi*, Si*	Chaotic cross-cutting gravels, pebbly sands and sands	Injection as sills/dykes due to intense over-pressure; also collapse and fill into fault-related open fissure
D4	Sd*, SFd*, Fd*	Disturbed sands and muds with slump folding	Soft sediment disturbance caused by slide-slump event
E1	C*	Calcrete at surface	Surface/soil cementation due to excess evaporation
E2	P	Paleosols and paleo-calcrete surfaces	Fossil soil and calcrete formation
F	L*	Micrites, muddy micrites and marls	Low energy, biogenic activity, lagoon/lake setting

Facies A2: Horizontal and cross-bedded gravels (Common occurrence) (Fig. 4A).

Bedding/structure: Medium to very thick-bedded units, with regular to irregular bedding, including wedge-shaped and lenticular bedding, sharp to gradational tops, sharp and erosive to gradational bases. Structured internal organisation and clast/grain fabric, with clear lamination, wavy lamination and cross bedding at a variety of scales – small-scale cross-bedded sets (0.1–0.15 m) to very large-scale cross-bedded units (up to 1.5 m), saucer-shaped lenticular bedding/lamination common. Oscillation grading is common within and between individual beds and sets.

Texture: Very variable grain size characteristics, poor to moderate sorting, pebbles typically 4–32 mm, sub-rounded to sub-angular, rarely with large angular to rounded clasts up to 500 mm in places.

Interpretation: High energy, deposition via traction, unidirectional fluid flow process, locally erosive; transverse and longitudinal bedforms, and/or upper-flow regime planar beds.

Facies A3: Structureless pebbly sands/sandy gravels (Minor occurrence) (Fig. 4A).

Bedding/structure: Generally thick-to very thick-bedded units with irregular to wedge-shaped bedding, sharp to gradational tops, sharp and erosive to gradational bases. Chaotic internal organisation and clast/grain fabric, with few clear sedimentary structures apparent, although indistinct oscillation grading is evident in some cases.

Texture: Very variable grain size characteristics, poor to very poor sorting, medium-coarse sand matrix, with pebbles typically 4–32 mm, sub-rounded to sub-angular, and rare larger clasts up to 450 mm.

Interpretation: High energy, rapid deposition, locally erosive; lag deposits, longitudinal bars, granular debris flows.

Facies A4: Horizontal and cross-bedded pebbly sands/sandy gravels (Common occurrence) (Fig. 4A).

Bedding/structure: Medium to very thick-bedded units, with regular to irregular bedding, including wedge-shaped and lenticular bedding, sharp to gradational tops, sharp and erosive to gradational bases. Structured internal organisation and clast/grain fabric, with clear lamination, wavy lamination and cross bedding at a variety of scales – small-scale cross-bedded sets (0.1–0.15 m) to very large-scale cross-bedded units (up to 1.5 m), saucer-shaped lenticular bedding/lamination common. Oscillation grading is common within and between individual beds and sets.

Texture: Very variable grain size characteristics, poor to moderate sorting, medium-coarse-sand matrix, pebbles typically 4–32 mm, sub-rounded to sub-angular, rarely with large angular to rounded clasts up to 45 mm in places.

Interpretation: High energy, deposition via traction, unidirectional fluid flow process, locally erosive; transverse and longitudinal bedforms, and/or upper-flow regime planar beds.

Facies B1: Structureless sands (Common occurrence) (Fig. 4B).

Bedding/structure: Generally medium to very thick-bedded units with irregular to wedge-shaped bedding, sharp to gradational tops, sharp and erosive to gradational bases. No sedimentary structures apparent, although in part this may be due to the highly unconsolidated nature of some outcrops that disintegrate on close inspection.

Texture: Mostly fine and very fine grained, with poor to moderate sorting. Isolated small pebbles relatively rare in occurrence.

Interpretation: Moderate-high energy, rapid deposition, locally erosive; longitudinal bars, channel-flood deposits.

Facies B2: Horizontal and cross-bedded sands (Very common occurrence) (Fig. 4B).

Bedding/structure: Thin to very thick-bedded units, with regular to irregular bedding, including wedge-shaped and lenticular bedding, sharp to gradational tops, sharp and erosive to gradational bases. Structured internal organisation and fabric, with clear lamination, wavy lamination and cross-bedding at a wide variety of scales and at a variety of levels of distinction. Oscillation grading is common within and between individual beds and sets.

Texture: Mostly fine and very fine grained, poor to moderate sorting.

Interpretation: Moderate-high energy, deposition via traction, unidirectional fluid flow process; transverse and longitudinal bedforms, and/or upper-flow regime planar beds; locally ripple-bedforms.

Facies B3: Bioturbated sands and muddy sands (Common occurrence) (Fig. 4B).

Bedding/structure: Thin to very thick-bedded units, with regular to irregular bedding, sharp to gradational tops, sharp and erosive to gradational bases. The principal structure evident is bioturbation, consisting of cylindrical, sub-vertical pipes of better-cemented sandstone. We interpret these as due to diagenesis associated with rootlet fill. In most cases these features are superimposed on whatever internal organisation, lamination and cross bedding that exist. Most typically, the rootlet bioturbation is evident as the bioturbation of sandy Facies B1 and B2, but also occurs as a less dominant part of the finer grained silt and mud facies (Facies C1 and C2), and within paleosol units (Facies E2).

Texture: Mostly fine and very fine grained sand, in some cases muddy sand, very poor to moderate sorting.

Interpretation: Rootlet bioturbation of fluvial sediments during periods of local non-deposition.

Facies C1: Silts (Minor occurrence) (Fig. 4C).

Bedding/structure: Thin to thick-bedded units, mostly with regular bedding, sharp bases and tops. Internal organisation and fabric, either with clear lamination, wavy lamination and cross-lamination at a variety of scales and at a variety of levels of distinction; or apparently structureless. Rootlet bioturbation traces locally present. Facies gradation occurs between silts and fine sands (B1, B2) on the one hand, and between silts and muds (C2) on the other.

Texture: Muddy silt to sandy silt, poor to moderate sorting.

Interpretation: Low energy, deposition from suspension and locally via traction, unidirectional fluid flow process where cross lamination is apparent.

Facies C2: Muds (Rare occurrence) (Fig. 4C).

Bedding/structure: Thin to thick-bedded units, mostly with regular bedding, sharp to gradational bases and tops. Internal organisation and fabric, either with minor lamination and wavy lamination (Facies C1 above), or apparently structureless. Rootlet bioturbation traces locally present. Facies gradation occurs between silts and muds (C1 and C2), and also between calcareous muds or marls and the micrites (muddy micrites) of Facies F.

Texture: Silty clay grade, poor sorting.

Interpretation: Low energy, deposition from suspension, and/or traction where lamination present, tranquil setting.

Facies D1: Chaotic clast-rich sands and gravels (Minor occurrence) (Fig. 4D).

Bedding/structure: Medium to very thick-bedded units, mostly with irregular bedding, including wedge-shaped, lenticular and mounded bedding, sharp to gradational tops, sharp and erosive bases. Structureless internal organisation and clast/grain fabric appears most common, but may also pass gradationally into identical facies showing lamination and cross bedding at a variety of scales. No evident grading, but some irregular grain-size variation may occur. This facies does not distinguish between the clearly finer-grained sands with abundant clasts, and the coarser-grained pebbly sands and gravels with abundant large clasts. In both cases, the clasts are dominantly pinkish to cream-coloured micrites and marlstones.

Texture: Very variable grain size characteristics, poor to moderate sorting, medium-coarse-sand matrix, pebbles typically 4–32 mm, sub-rounded to sub-angular, with abundant to common, angular to rounded, exotic large clasts up to 550 mm diameter.

Interpretation: High energy, deposition from debris flows, probably locally derived, presumed fluvial.

Facies D2: Disturbed sands with chaotic or contorted lamination (Rare occurrence) (Fig. 4D).

Local occurrence of highly disturbed sands, either with chaotic/contorted lamination.

Interpretation: contorted lamination due to disturbance of unconsolidated wet sediment caused by seismic tremor or sudden debris flow event.

Facies D3: Chaotic cross-cutting gravels, pebbly sands and sands (Rare occurrence) (Fig. 4D).

Local occurrence of highly disturbed pebbly sands and gravels, cross-cutting adjacent facies.

Interpretation: sand/gravel injection (clastic sills and dykes) due to intense over-pressure; and collapse and fill into fault-related open fissure.

Facies D4: Disturbed sands and muds with slump folding (Rare occurrence) (Fig. 4D).

Local occurrence of disturbed sands and sand/mud units, with tightly overturned-fold characteristics. Discontinuity surfaces cross-cutting normal stratification also occur, with little other deformation apparent.

Interpretation: soft sediment disturbance caused by slide-slump event; units with little internal deformation and a basal slide-plane discontinuity surface due to sliding.

Facies E1: Calcrete (Common/minor occurrence) (Fig. 4E).

There is an almost ubiquitous occurrence of a hardened, calcite-cemented, surficial layer of variable thickness (typically 0.5–1.5 m, but up to 2.5 m maximum). This shows a pervasive and aggressive carbonate cement at and below the outcrop surface – through sands, pebbly sands, gravels or other facies. Much of the structure and fabric of the original facies has been obscured by cementation, although grading and indistinct lamination are locally visible. Irregular carbonate nodules and calcretised rootlet traces occur locally.

Interpretation: surface calcrete results from excess evaporation

over precipitation, typically in arid/semi-arid environment, during period of non-deposition; thicker developments of calcretised horizon indicate prolonged periods of non-deposition.

Facies E2: Paleosol horizons and paleo-calcrete surfaces (Rare occurrence) (Fig. 4E).

Within-formation horizons occur that we interpret as the result of paleosol and paleo-calcrete development. Paleosols show reddening of the sand/silt/mud facies, minor rootlets and locally carbonate nodules. Paleo-calcretes show hardened, calcite-cemented, pale-coloured horizons, in some cases underlain by reddened paleosols, rootlet traces and carbonate nodules. Within-formation paleosols and paleo-calcretes are typically relatively thin (0.1–0.3 m) and more rarely up to 0.8 m thick.

Interpretation: normal soil formation during period of non-deposition (locally or regionally).

Facies F: Micrite, muddy micrite, marlstone (Rare occurrence) (Fig. 4F).

Bedding/structure: Thin to medium-bedded units, mostly with regular bedding, locally lenticular, sharp to gradational bases and tops. Internal organisation and fabric apparently structureless. Rootlet bioturbation traces are locally present. This is a rare, locally occurring facies of true limestone (micrite/marlstone) within the otherwise siliciclastic-dominated facies suite. Facies gradation occurs between this facies and the silt/mud facies (C1/C2), and the paleo-calcrete facies (E2).

Texture: Silty clay (micrite) grade, poor sorting.

Composition: Carbonate-rich, limestone facies.

Interpretation: presumed local development of lagoonal sedimentation in overbank lagoon/lacustrine setting; this facies needs further investigation.

5.3. Facies associations and environmental interpretation

Six distinct facies associations (FA1 to FA6) can be identified in the field, based on their common co-occurrence both in vertical section and lateral juxtaposition. These are summarised in Table 4, together with a preliminary interpretation of their likely depositional environment.

The principal evidence for a mainly fluvial interpretation of the facies and facies associations encountered in both Pliocene and Quaternary successions is the following:

No marine macrofossils have been found in the field, and no microfossils are present in the (limited) laboratory examination of the fine-grained facies. There is rare woody debris present in some localities.

There are clear rootlet traces present at some localities, and common paleosol horizons with reddened horizons, calcrete surfaces and caliche nodules.

The Quaternary succession occurs in clear river terraces, on several levels, adjacent to the modern Euphrates.

The Pliocene succession, which was studied in detail, lies close to the present Euphrates River, but has undergone tectonic uplift. It rests unconformably on the Lower Miocene gypsiferous Lower Fars Formation and represents the influx of coarse-grained terrestrial sediment following a period of uplift and erosion.

Most of the facies (gravels and sands) are best interpreted as the result of moderate and high-energy depositional processes, and many with parallel and cross-bedding indicative of unidirectional flow and traction-current deposition. Others, such as the massive gravels and chaotic facies are typical of flood deposition, debris flows, and bank collapse. The fine-grained facies are all typical of lower-energy flows and deposition from suspension/traction, commensurate with overbank and flood plain environments.

Most of the facies associations identified (Table 4), as well as the bedforms, architectural elements and vertical facies sequences documented in the field (see 5.3 below) are best interpreted as from fluvial depositional environments (e.g. Miall, 1996, 2010).

There is some evidence for deposition in other related continental environments. The rare limestone/marl facies, encountered *in situ* and as reworked intraclasts, might be of lacustrine origin, possibly ephemeral shallow lakes on the river flood plain. Where there are abundant debrites, other chaotica and gravels, may indicate local alluvial fans marginal to the main river and flood plain.

5.4. Architectural elements

5.4.1. Element recognition

By recognising the common association of certain facies, inferring the likely depositional processes based on facies attributes (as above), and setting these within the context of vertical logs measured at each site (Figs. 5 and 6), we can make environmental interpretations of distinctive architectural elements common in fluvial systems.

Good outcrop exposure allows documentation of the lateral context of these facies associations and vertical sequences, through measured field sketching and interpretation of multiple photo

Table 4
Characteristics and depositional environment interpretations of the six distinct facies associations (FA1 to FA6) identified in the study area of Syria.

Facies Association FA1
Facies: Dominance of gravels and pebbly sands (Facies A1, A2, A3, A4), with common sands (B1, B2), and minor chaotica (D1, D4).
Interpretation: These typically occur in high-energy channels or braided channels.
Facies Association FA2
Facies: Dominance of sands and muddy sands (Facies B1, B2), with variable amounts of gravels (A3, A4) muddy sands (B3), fine-grained sediments (C1, C2), and chaotica (D1, D4).
Interpretation: These typically occur in low-energy channels or meandering channels.
Facies Association FA3
Facies: Dominance of sands and fine-grained sediments (Facies B1, B2, B3 and C1, C2), with minor paleosols (E1, E2), and rare limestones (F1).
Interpretation: These commonly occur overlying FA1 and FA2 and are typical of the final fill phase of abandoned channels.
Facies Association FA4
Facies: Co-dominance of debrites (Facies D1) and sands (Facies B1, B2, B3), with minor fine-grained facies (C1, C2), and other chaotica (D2, D4).
Interpretation: These we interpret as representing small-scale cut-and-fill channels.
Facies Association FA5
Facies: Co-dominance of sands (Facies B2, B3) and fine-grained sediments (Facies C1, C2), with common paleosols (E1, E2), and rare limestones (F1).
Interpretation: These typically occur as flood-plain or overbank deposits.
Facies Association FA6
Facies: Dominance of sands (Facies B1, B2, B3), with silts (Facies C1), locally occurring within FA5 flood plain deposits.
Interpretation: These are interpreted as crevasse splay units.

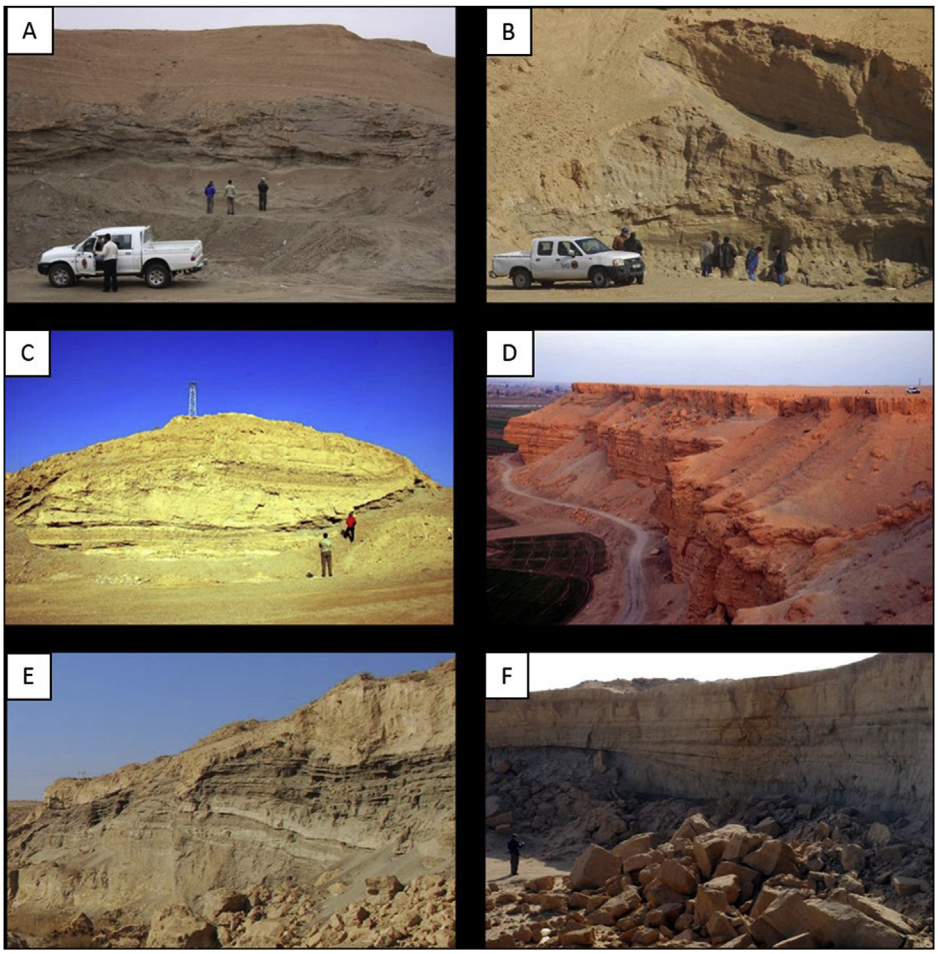

Fig. 5. Field photographs showing the key localities described in this paper; A) Al Rabah quarry section, B) Ain Ali roadside section, C) El Ward quarry section, D) Dweir platform margin, E) Ayash Quarry, F) Al Khawr Quarry.

panels (Fig. 7). The lateral extent observed is from 50 m to over 1000 m, and vertical extent from 5 to 50 m. These observations confirm the presence of channel incision, channel margin and overbank, and allow good estimation of element architecture and dimensions.

5.4.2. Channel architecture

The channel elements identified include (Fig. 7): (a) broad, high-energy, gravel-rich, probably braided-river systems; (b) medium-scale, lower-energy, mixed-fill, probably meandering-river systems; and (c) small-scale, deep-incision (cut-and-fill) channels, characterised by common mass flow facies. Channel widths, where these can be measured or inferred, range from 100 m to 500 m, 50 m–150 m, and 30 m–60 m, respectively, for these three different channel types. Depths of fill range from approximately 3 m to a minimum fill of 7 m for an individual channel segment. The maximum fill thickness is mostly obscured by subsequent erosion or lack of exposure. Stacked channel units (involving at least two channel bodies) can be inferred in places, with combined fill thickness up to 25 m.

The sediment fill of the braided systems is mainly gravel-rich (FA1), with a blocky to fining-upward vertical sequence, locally passing upwards into abandoned channel (FA3) or overbank (FA5) facies, over an incised channel margin and erosive base. The sand/shale ratio is > 9:1, with no widespread barriers, and few localised baffles to flow. However, there is significant lateral and vertical facies variation, with evidence for large and small-scale migrating bedforms, sand and gravel bars from 10 to 50 m long, shallow-dipping lateral accretion surfaces most likely related to point-bar deposition, and marginal bank collapse as evidenced by localised debrites comprising angular and distorted clasts of overbank facies. Where it has been possible to infer channel orientation is mostly NW-SE or N-S. More than 100 measurements of cross-bedding also show a dominant SE flow direction, with a 90^0 spread about this mean.

The lower-energy or meandering channels are characterised by sand-rich facies (FA2), with a blocky and fining-upward vertical sequences both common, over incised channel margins and an erosive base. The abandoned channel and overbank facies associations may be relatively thick within the channel, in some cases. The sand/shale ratio is between 7:1 and 9:1, with none or few barriers, and few but thicker baffles to flow. A range of small to large-scale migrating bedforms is evident, as well as marginal bank collapse. Channel orientations are mainly NW-SE, but with a wide spread of flow directions ($0\text{-}180^0$) derived from more than 150 cross-bedding measurements.

The small-scale cut-and-fill channels have common debrites (facies D1) within an otherwise sand-rich facies, and no evident systematic vertical sequences. The debrite matrix is mainly sandy, so that sand-shale ratios are high (>8:1), but some clays and/or carbonate cement within the debrites may cause local flow baffles. No systematic flow directions could be determined.

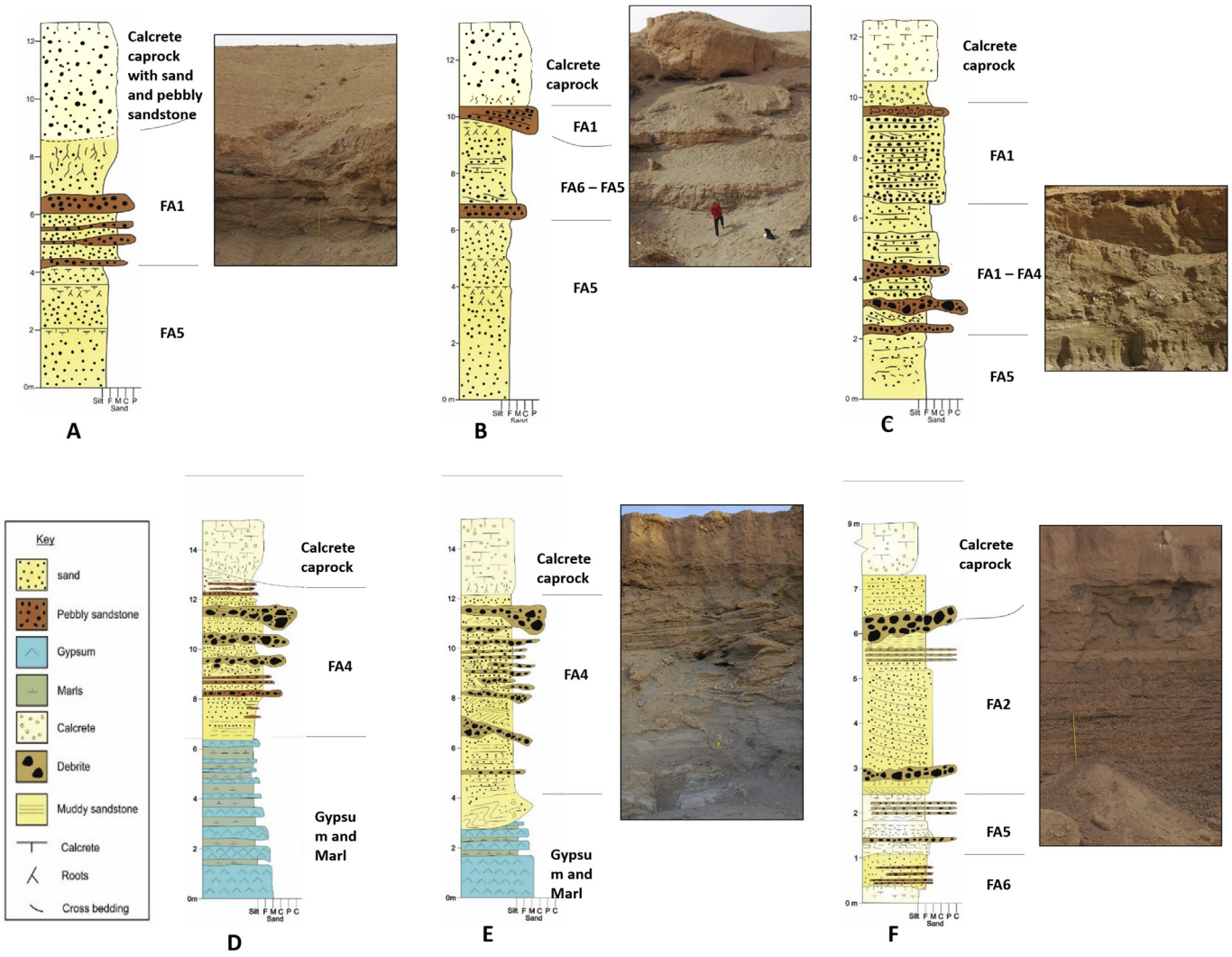

Fig. 6. Vertical sedimentary logs measured through selected outcrop sections of Pliocene (Mayadin formation) and Quaternary (Al Furat formation). Relevant facies associations indicated, together with section or part-section field photos. A, B: Al Rabah Castle section; C: Ain Ali Roadside; D, E: Dweir platform margin; F: El Ward Quarry.

Lateral correlation of channel architecture can be made over at least 1 km with certainty, for some of the outcrops studied, and inferred over a much greater area. In general, it appears that Al Furat Group (Quaternary) channels migrated rapidly and extensively over a wide area. This may have been equivalent in width to the flood-plain of the present-day Euphrates River plain, which is up to 10 km wide in places. These Quaternary high-energy river channels built up a laterally persistent coarse-grained, channel facies association – both across flow and parallel to flow. The Upper Pliocene Mayadin Formation channels present a wholly different aspect, probably with smaller channel elements in an extensive sheet sand system. However, this preliminary interpretation needs further study.

There is an overall upward coarsening of facies from the underlying Miocene to Lower Pliocene Doura Europos Formation (gypsums, mudstones and marlstones), for which we do not see any evidence of a fluvial channel system, through the Upper Pliocene Mayadin Formation, to the Quaternary Al Furat fluvial system. The topmost part of the Quaternary system becomes slightly finer grained in the studied localities, and the present-day Euphrates River sediments appear still finer grained on average.

5.4.3. Flood plain/crevasse splay architecture

We recognise both flood plain and crevasse splay elements inferred from Facies Associations and outcrop architecture (Figs. 6 and 7), although these are very difficult to distinguish in terms of plan geometry in the field. The flood plain extent and thickness are presumed to be greater than those of the channels, although the succession is less well preserved in the record and/or less well exposed. Flood plain deposits are characterised by fine-grained sands, muddy sands, silts and muds (FA5), with evidence of rootlets and paleosols. The sand/shale ratio is between 4:1 and 6:1, with some mud-rich potential barriers, and common baffles to flow.

Crevasse splay lobes can be recognised as individual elements within the flood plain succession adjacent to and underlying principal channel elements. Those identified show an approximate width of 30–60 m, and maximum thickness of individual sand units (i.e. lobe crest) of 0.5–1.5 m. It was not possible to ascertain their areal extent. They are more distinctly sand-rich (FA6) than the flood plain deposits, with a typical sand/shale ratio 6:1 to 7:1.

5.5. Synsedimentary tectonic features

There are several lines of evidence that neotectonic activity over the past 3 Ma has affected both sedimentation and architecture of the Euphrates river system. The principal features observed are the following.

River terraces: As outlined in Section 4 (Table 2), five earlier terraces are recognised prior to the present one (Trifonov et al., 2011). These have been recently dated to around 0.4 Mya (7–15 m above present floodplain), 0.7 Mya (15–25 m), 1.6 Mya (30–45 m), >2.12 Mya (45–60 m) and >2.8 Mya (80–100 m). If we discount sea-level changes, this could be accounted for by a stepped uplift at a mean rate of 25–30 m/Mya during this period of time, leading to river incision of up to 100 m. As there is no clear correlation of terrace dates with sea-level lowstands, we infer a mainly tectonic control on their development.

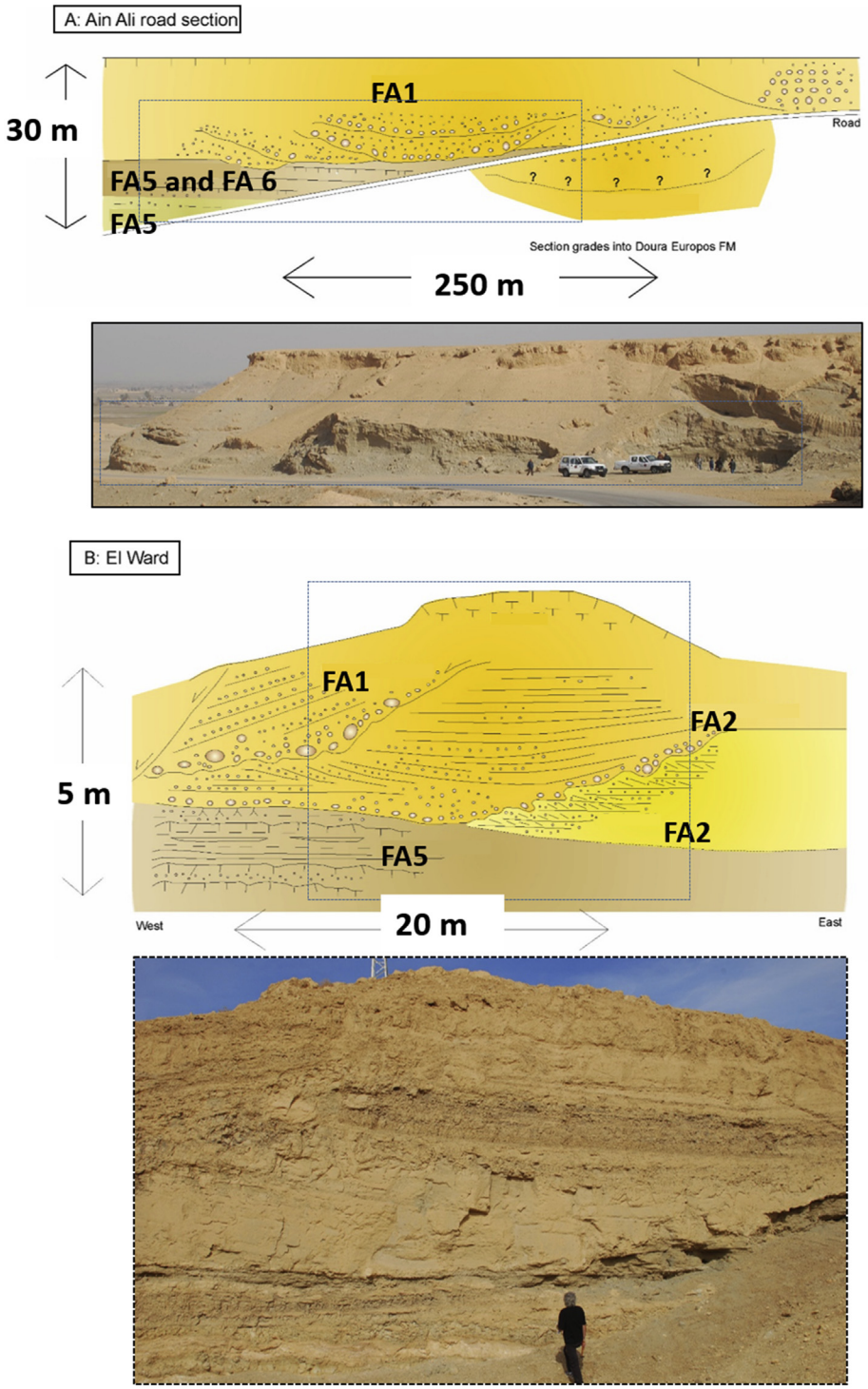

Fig. 7. Selected field sketches showing lateral distribution of facies and architectural elements observed and measured from key field localities. Relevant facies associations indicated, together with section or part-section field photos. A: Ain Ali Roadside, late Pliocene; B: El Ward Quarry, late Pliocene; C-F: Al Khawr Quarry, Quaternary.

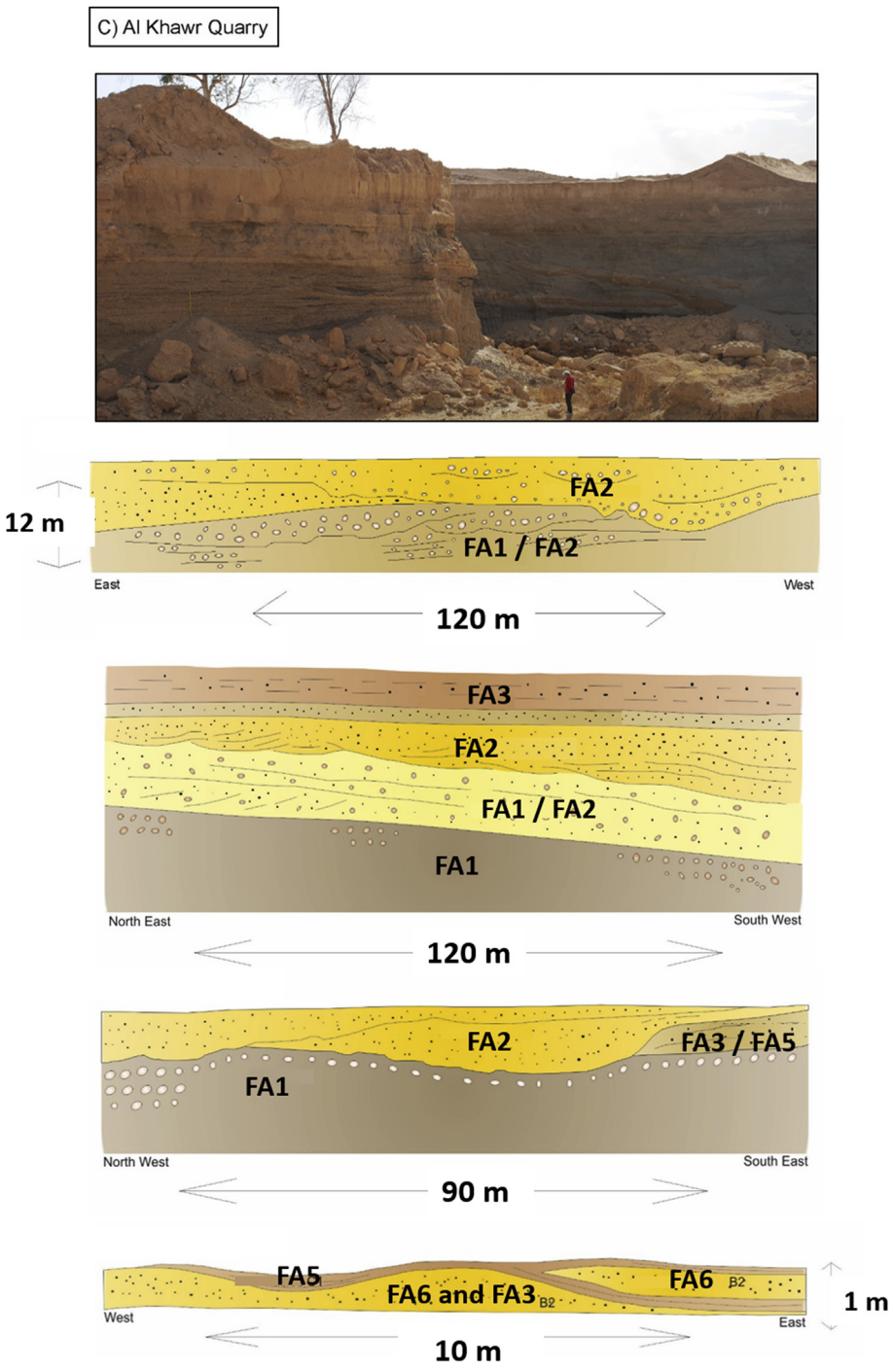

Fig. 7. (*continued*).

Gravel pipes: Within the Quaternary section at Ayash Quarry locality, there are vertical gravel pipes that become funnel-shaped upwards. The pipe structures cross-cut the normal (horizontal) bedding and are filled with gravels and pebbly sands (maximum clast ~2 cm; modal clast size ~1 cm), having a chaotic clast fabric. They range from 5 m to 11 m in length and 0.3 m–0.5 m in diameter, or up to 1–1.4 m diameter at the top of the funnel portion. The pipes may have formed due to neotectonic fissures opening as a result of extensional tectonics and being filled from overlying unconsolidated gravel into the underlying sand beds. Alternatively, they might represent ice wedge and fill structures.

Sand dykes: Minor sand injection through irregular-shaped dykes and sills into adjacent or overlying strata is present at several localities. Such injectites are typically related to intense overpressure of unconsolidated wet sands as a result of sediment overburden. However, the Quaternary and Pliocene sands in this study area have never been buried by more than a few tens of metres at most, so that sand injection is more likely due to sudden faulting and fluid pressure release from depth. The injectites observed are all closely linked to reverse faults.

5.6. Modern Euphrates system

The modern Euphrates River is in its middle reaches through the study area from Al Raqqa to the Syria/Iraq border. The average gradient in this section across the Syrian uplands is approximately 0.6 m/km. This compares with the upper reaches of the Euphrates in Turkey, where the average gradient is around 3.5 m/km, and the lower reaches across the plains of central Iraq, where the gradient is < 0.06 m/km. The middle reaches are characterised by an actively flowing channel, mostly between 100 and 300 m wide, but reaching up to 500 m in parts and less than 50 m where it has divided into two or more strands. The river has parts that are tightly meandering, parts that are low-sinuosity braided channels and parts that are anastomosing.

In braided sections, there are a range of elongate braid bars, the more prominent ones of which have grown into ephemeral islands several hundreds of metres in length and tens of metres in width. Meandering segments show the development of major point bar sequences, and common abandoned channels and meander loops. Crevasse splay deposits are seen locally, but are generally more difficult to observe beneath the agricultural or urban development over much of the flood plain. This flood plain is mostly 5–7 km wide, reaching in excess of 10 km in parts and narrowing to less than 0.5 km through the Halabiyah Gorge, north of Deir-ez-Zur.

The modern river valley in the study area is clearly constrained by a faulted basin margin along part of its southern edge, where the channel is very straight and closely follows the fault. Only one sizeable tributary joins the Euphrates in this section, near Al Busayrah, some 20 km south of Deir-ez-Zur. However, there are several other short-headed dry river valleys (wadis), particularly along the southern margin. Upstream of the study area, the river course has been modified by the Tabqa dam. Prior to the river modification by a series of upstream dams, the estimated water discharge was around 600–800 m^3/s carrying up to 1 tonne/s of sediment load.

The sedimentary deposits related to the modern Euphrates River channels are dominated by moderate to well-sorted, massive, cross bedded, trough cross-bedded and parallel-laminated sands. The sands range between fine grained and coarse grained, representing the different flood cycles of the river system. Flood plain deposits are mainly muds and silts, with extensive soil formation, red staining and rootlet bioturbation. These are mostly obscured and modified by use for agriculture and urban development.

6. Discussion

6.1. River system development

Fluvial deposits in the Euphrates valley in this part of Syria record the development of the Euphrates River system from the Pliocene through to the present day. The summary palaeogeographic maps in Fig. 8 also show the precursor of mid and late Miocene geographies, based on previous literature (Fig. 8a, b).

The Upper Pliocene fluvial deposits represent an early stage of the Euphrates River (Fig. 8c), which may have included a paleo-trunk river as well as an alluvial-fluvial fringe of sediment derived from an area or areas of active tectonic uplift prior to and during deposition. In the outcrops examined the Pliocene fluvial system is represented by a series of relatively small and probably short-lived river channels, with local debrites and sand to mud fill. We interpret these systems as representing early consequent drainage systems that formed in an underfilled foreland basin, shortly after the final closure of the last of the Tethyan seaways in this area. These were likely relatively short fluvial systems draining the Tethyan orogens to the north and northeast, flowing into and progressively filling a marine basin with a shoreline that was most likely located somewhere around the Syria-Iraq border. The smaller cut-and-fill channels, noted especially at the Dweir locality, are interpreted as representing local wadi tributary valleys.

The Pleistocene system (Fig. 8d) represents a moderate to large river, probably following in a similar broad valley as the present-day Euphrates. By this stage, it had evolved into a larger-scale and more integrated system than the small channels of the Pliocene. It is inferred to have been a relatively higher energy system than at present, with equal to larger dimension architectural elements and typically coarser grain size of sediment. It underwent several adjustments and reactivations, possibly as a result of sea-level change, and has also been locally affected by neotectonic activity. The grain size and facies associations present indicate that this was a largely braided or anastomosing channel belt, perhaps with some meandering sections, which rapidly migrated across a broad floodplain. This implies that either the river gradient, or its discharge and sediment load, were higher than the modern river. We interpret this as being due in part to more active tectonic uplift in the hinterland, and in part to the shorter distance between the hinterland and the coastline, which was likely around 2000 km at this time (Fig. 8d).

A change to a finer grain size can be seen towards the surface of the Quaternary deposits, from gravel at the base to coarse/medium sands at the top. This probably marks the onset of a slowdown in tectonic uplift and/or a rise of base level. The present-day system (Fig. 8e) is represented by finer grained sands, silts and muds. This may reflect continued decrease in tectonic activity and the rate of hinterland uplift. However, the Euphrates River has also been considerably modified upstream of the study area by a series of dams, which have regulated flow discharge.

6.2. Depositional controls on facies architecture

In section 6.1 (above), we discussed the vertical change in fluvial facies observed along the middle reaches of the Euphrates River, in central and southern Syria. There is a clear trend from small-scale channels and medium to coarse-grained deposits in the Upper Pliocene, to large-scale, coarse-grained (gravel-rich) braided and anastomosing channels in the Pleistocene, and finally to the modern river, which is interpreted as lower energy than that of the Pleistocene, and which has incised the earlier channel and flood plain deposits in the field location. In this section, we discuss a number of possible models and controls that might explain this change in fluvial facies, based on the sedimentary evolution of the whole fluvial system in its tectonic context.

Model 1: stream lengthening due to infill of accommodation space in the foreland basin

Palaeogeographic reconstructions clearly indicate that the shoreline of the Persian Gulf and the delta of the Euphrates-Tigris-Shatt-al-Arab system have moved to the south and east through time. Middle Miocene successions in the north of Syria indicate that there were marine conditions in the region until that time, whereas marine conditions in the east of Syria and northern Iraq continued until the Pliocene. The 800–1000 km shift in shoreline position from the late Pliocene to present day would have resulted in a corresponding increase in stream length and, assuming that the elevation of the hinterland remained nearly constant and that there was no change in base level, this would have resulted in a significant decrease in the average gradient of the river.

Model 2: response to large base level changes, exaggerated by restricted marine conditions in the Persian Gulf

Although the Zagros deformation front has roughly propagated

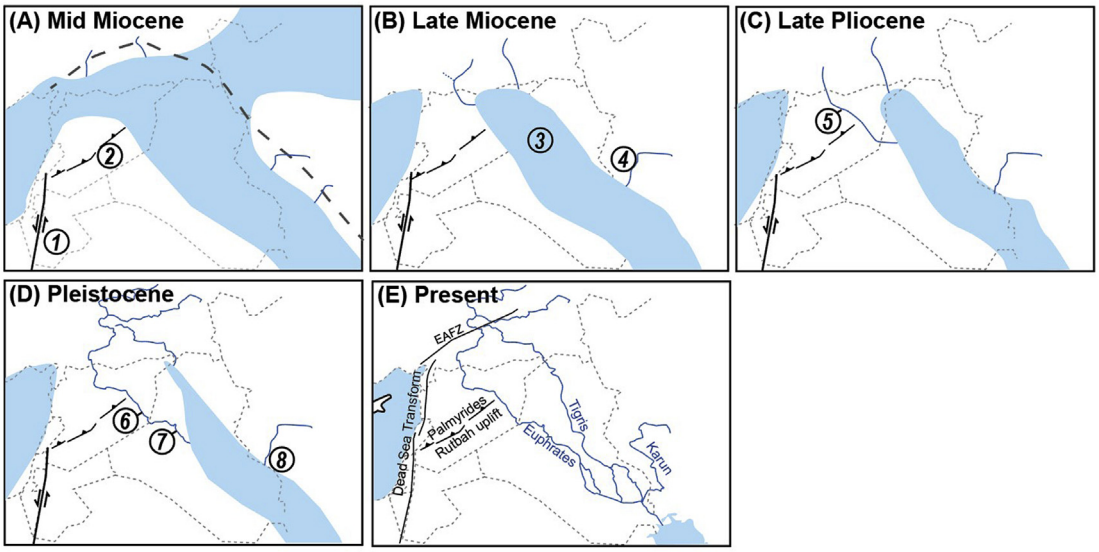

Fig. 8. Palaeogeographic reconstructions of the Euphrates river system from mid-Miocene to Recent. Blue polygon shows seas/lakes and light blue dashed line shows suture between Eurasian and Arabian plates. (A) Mid Miocene – continuous seaway from the Mediterranean to the Arabian Sea. Consequent drainage systems form in the uplifting Tauride and Zagros mountains to the north and east of the seaway. *(1)* Propagation of the Dead Sea Transform to the restraining bend in Syria by 17.1–12.7 Ma (Nuriel et al., 2017) resulting in *(2)* the onset of transpression in the Palmyrides (Brew et al., 2003). (B) Late Miocene – closure of seaway between Mediterranean and the formation of the proto-Persian Gulf, *(3)* resulting in widespread deposition of restricted marine evaporites (Lower Fars Formation). *(4)* Deformation propagates eastward in the Push-e Kush Arc by the Tortonian. (C) Late Pliocene – fluvial-deltaic sediments begin to fill the Mesopotamian foreland, resulting in longer, more integrated fluvial systems. *(5)* River terraces form in Central Syria. (D) Pleistocene – evidence for uplift of river terraces in SE Syria (*6*) (Trifonov et al., 2012) and (7) NW Iraq (Demir et al., 2007), which include gravel derived from Anatolia. *(8)* Coarse-grained alluvial-fluvial sediments (Bakhtyari Formation) from the Zagros continue to be deposited on the eastern shores of the Persian Gulf. (E) Present – Fully integrated Shatt-al-arab river enters the Persian Gulf downstream of the confluence of the Euphrates, Tigris and Karun rivers.

from NW to SE since the initial collision in the region of eastern Turkey, irregularities in the shape of the leading edge of the Arabian Plate mean that the migration of the deformation front has not been uniform. This is particularly evident from the present day geometry of the plate boundary, as the promontory represented by the Musandam Peninsula (near the Strait of Hormuz) has led to increased deformation and rapid Pleistocene-Recent surface uplift in this area (Wood et al., 2012), resulting in a restricted marine connection between the Persian Gulf and Arabian Sea. During glacial sea-level lowstands, emergence of this narrow sill led to isolation and desiccation of the Persian Gulf, followed by periods of inundation during marine transgressions. This has had a significant impact on the local landscape, climate and even early human migration and settlement (Rose et al., 2010) but will also have had a very significant impact on the location of the delta, and the base level upstream of the river mouth.

During lowstand periods, when the Persian Gulf was desiccated, the Shatt-al-Arab river (now connected to the Euphrates and Tigris rivers that rise in the Zagros Mountains) would have flowed across the entire Persian Gulf and deposited its water and sediment load directly into the Arabian Sea. This would also have been accompanied by an upwards migrating drop in base level, represented by knickpoint propagation and a corresponding phase of incision in some fluvial reaches, and an increase in gradient in other reaches. An increase in gradient may have led to changes in sedimentary facies from lower-energy (meandering) to higher energy (braided) systems in the middle reaches. Subsequent marine transgressions would have had the opposite effect, raising base level, reducing the average gradient of the river, and a corresponding shift in sedimentary facies.

Model 3: migration of forebulge unconformity and intraplate deformation

Isopach and sedimentary facies maps from subsurface seismic and well data (Litak et al., 1997) show a change in the position of the main depocentre of the foreland basin from the NW to the SE through time. Uplift and incision of older fluvial deposits and their floodplains has also been diachronous, with fluvial terraces in northern Syria dated as Pliocene in age, and terraces to the south, in SE Syria and NW Iraq, of Pleistocene age (Demir et al., 2007; Trifonov et al., 2013). These are the same terraces that have uplifted and exposed the sediments analysed in this study. This NW to SE propagating uplift and corresponding shift in foredeep depocentre most likely represent the migrating forebulge of the Zagros Mountains as the deformation front moved to the SW. Alternatively, or in part, it may be linked with uplift of the Palmyrides. As observed in the present-day river system, the fluvial morphology changes significantly between the middle reaches in Syria and lower reaches of the river in northern Iraq, where the river changes gradient by about a factor of 10, from 0.6 m/km to 0.06 m/km in front of the present-day forebulge. Intraplate deformation as a result of uplift of the Palmyrides, and reactivation of the Rutbah Uplift, has also resulted in surface uplift of the central part of the northern Arabian Platform. The change in facies observed in the middle reaches may, therefore, partially represents a change in sedimentary facies in front of the south-easterly migrating forebulge and Palmyrides surface uplift since the Pliocene.

Model 4: integrated fluvial and geomorphological evolution

The evolution of the Tigris and Euphrates River system has responded to a number of different factors, including base level change, stream lengthening (and a corresponding change in gradient), and the intraplate deformation associated with orogenesis to the north and east (forebulge migration) and changes in tectonic boundary conditions to the west. Although it is difficult to disentangle the effects of these competing depositional controls, we believe that the facies transitions and architectural evolution observed in the field primarily represent a combination of drainage integration, stream lengthening, and regional uplift of the middle reaches of the Euphrates River and its precursors. The number of

different factors, however, highlights the complexity of drainage evolution in tectonically active basins, as seen in other systems worldwide (Wheeler and Cook, 1954; Clark et al., 2004; Nicholson et al, 2014, 2016, Nicholson et al., 2019), and the need to consider multiple competing factors when assessing fluvial systems in their sequence stratigraphic and tectonic contexts.

6.3. Significance for reservoir modelling

Large-scale effects

The results presented here provide quantifiable data on the sedimentary facies and architecture of a well-exposed Pliocene-Quaternary fluvial system. This adds, therefore, to the compendium of analogue data for use in understanding and modelling of subsurface reservoirs. The data are from the middle reaches of a moderate to high-energy, continental-scale river system. Channel widths, where observed, ranged from 50 m to 500 m for the different channel types, with depths of fill ranging from approximately 3 m to a minimum fill of 7 m. One problem for identifying the maximum fill of a channel was lack of preservation of the section and erosion by subsequent channelling. Where stacked channels were observed, combined fills of up to 25 m thick were observed.

Lateral correlation can be made over at least 1 km with certainty, and inferred over a much greater area. In general, it appears that Quaternary Al Furat Group channels migrated rapidly and extensively over a wide area, equivalent to the modern day Euphrates River plain, and so were able to build up a laterally persistent channel facies association, both across flow and parallel to flow. The Pliocene Mayadin Formation channels present a wholly different aspect, with smaller channel elements in an extensive sheet sand system. Crevasse spray lobes can be identified as individual elements within the overbank successions adjacent to and underlying the principal channel elements in Quaternary (Al Furat) deposits. Those identified show an approximate width of 30–60 m and maximum thickness of individual sand bars and down-flow braid bars are identified as separate bodies. These range up to 20 m in cross-channel or down-channel extent, and from 1 m to 3 m in thickness. The proportion of channel sandstones in the overall stratigraphy of the paleo-river valley is difficult to assess with accuracy, due to the limits of outcrop dimensions and the tendency of finer floodplain sediments to be weathered and so not crop out so well, thus leading to a bias towards inferring a greater sandstone proportion. However, when large outcrops are seen (for example in quarries, Fig. 5), the proportion of channel sandstones is in the range of 65%–95%. This suggests that the channels will be well connected (David and Hovadik, 2006) and so recovery factors are likely to be good. This depends, of course, of the nature of channel-to-channel contacts. At outcrop, in some multistorey/multilateral sandbodies, individual channels are seen to have good sand-on-sand contacts, but others are marked by abundant mudstone, siltstone and carbonate intraclasts (e.g. Fig. 5B and C). In the latter cases, the intraclasts would tend to form a baffle to fluid flow.

In terms of potential reservoir attributes, it is clear that the higher-energy gravel/sand-rich systems of the Quaternary Euphrates represent very good potential – broad channel facies, extensive lateral migration, and high net-to-gross. Interbedded mudstones and siltstones are relatively minor and present only localised baffles to fluid migration. The heterogeneity of the reservoir facies suite (gravels and sands), however, would need to be carefully mapped and modelled in order to maximise production (see below). By contrast, the lower-energy Pliocene river system would offer less favourable reservoir potential – restricted width/depth channels, localised migration, and moderate net-to-gross fill. A higher proportion of mud/silt facies, as well as matrix-rich debrites, would further mitigate against a productive reservoir. These differences are clearly linked to overall evolution of the drainage system within the Mesopotamian foreland basin. Although we have discussed three different models that may have led to this evolution, our field data does not allow us to differentiate between models, nor to gauge which system might be more or less beneficial to future reservoir potential. However, assessment of fluvial and geomorphological evolution and their controls is nevertheless an important element to understand for any subsurface system.

Small-scale effects

On a smaller scale than the overall channel scale, the beds and lenses of sandstone which are commonly observed in some of the gravel-dominated channels would have a significant impact on reservoir behaviour (Fig. 9). In most cases, the matrix of the gravel/conglomerate consists of a similar grain-size and sorting to the sandstone lenses and beds. Because of this, the sandstones will have a higher porosity and permeability than the gravels, so that, in a producing reservoir, much of the fluid flow might be concentrated in the sandstone units. The higher flow rate should be visible if a production logging tool (PLT) is run and laterally-restricted sandstone lenses might also be visible on a well test as negative skin . A combination of well testing and PLT might allow lenses and beds of sandstone, within a gravel-dominated channel system, to be identified and differentiated. Their presence can then be accounted for in any reservoir modelling, leading to a better understanding of likely reservoir behaviour.

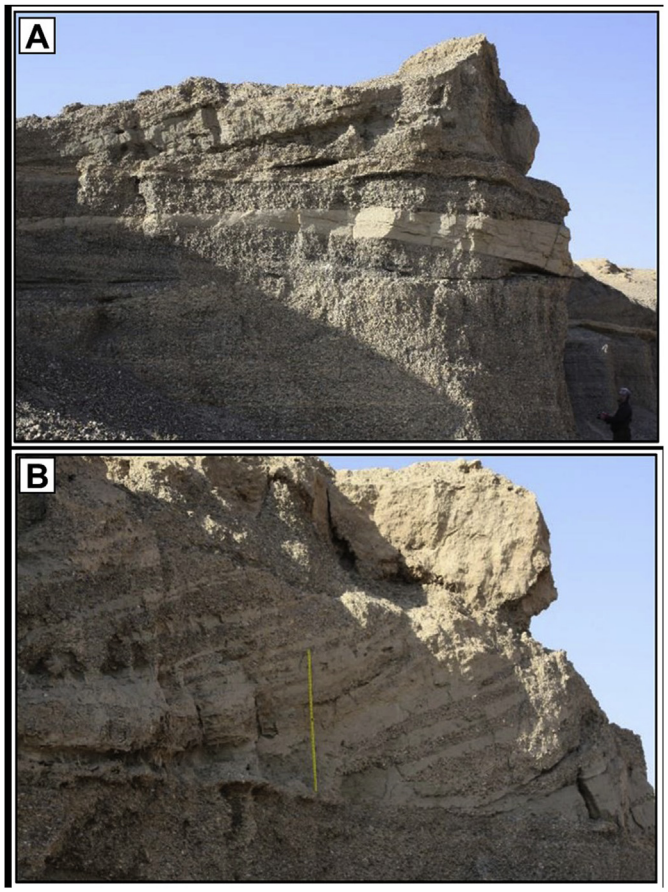

Fig. 9. Detail of Quaternary fluvial channel architecture seen in outcrop photographs from El Khawr Quarry. (A) Lenticular sandstone body and large-scale cross-bedding within a gravel-rich channel-fill; (B) Large-scale cross-bedding showing alternation of gravel and sand in dune foresets.

7. Conclusion

This paper provides the first detailed study of the sedimentary characteristics of Upper Pliocene and Quaternary fluvial deposits along the middle reaches of the present-day Euphrates River, from the city of Al Raqqa to Al Bukemal, near the Syrian-Iraq border. The Tigris-Euphrates is a large-scale fluvial system, draining over 1 million km^2 of SW Asia. It originated in the Late Miocene and developed into the principal axial drainage system of the region, following the broad structural features of the Mesopotamian Foreland Basin. The principal findings of this study are as follows:

The Pliocene fluvial system is characterised by small, isolated, cut-and-fill channels, with abundant debrite and slump facies. The Quaternary system, by contrast, shows broad channels with extensive lateral migration across at least 1 km of flood plain.

The principal Quaternary facies include gravels, pebbly sands and sands as channel associations, coupled with sands, muds and paleosols representing channel abandonment, overbank and crevasse-splay associations. Channel widths range from 50 m to 500 m, and minimum fill thicknesses from 3 m to 7 m. The combined channel-fill for stacked channels is up to 25 m thick. Smaller-scale crevasse splay lobes in the overbank deposits have widths of 30–60 m and sand thickness of 0.5–1.5 m.

The geometry, facies characteristics and dimensions of these architectural elements provide a useful quantifiable analogue for subsurface reservoirs. Clearly, the Quaternary-style fluvial system would provide more favourable reservoir attributes than those of the Pliocene in terms of both facies attributes and geometry. The high-energy channel facies show generally very good reservoir attributes, with good correlation and connectivity. At the small (bed) scale there is significant heterogeneity of characteristics that would impact fluid-flow through the formation in the subsurface. Controls on system evolution are a complex interplay of drainage integration, stream lengthening and regional tectonic uplift.

Declaration of competing interest

The authors declare that they have no known competing financial interests or personal relationships that could have appeared to influence the work reported in this paper.

Acknowledgements

We gratefully acknowledge funding and logistical support from Shell Syria, Shell Development Oman, and Petroleum Development Oman. Field support was provided by colleagues from the University of Damascus (Syria), Al Furat Petroleum Company (AFPC) and the Syrian Petroleum Company (SPC). The University of Damascus (Syria) and the Institute of Petroleum Engineering at Heriot-Watt University (UK) provided all necessary administrative support throughout.

References

Adeloye, A.J., Soundharajan, B.-S., 2019. Effect of dynamically varying zone hedging policies on surface water reservoir operational performance during climate change. Geol. Soc. of London Special Publ. 488, 277–289.
Agard, P., Omrani, J., Jolivet, L., Mouthereau, F., 2005. Convergence history across Zagros (Iran): constraints from collisional and earlier deformation. Int. J. Earth Sci. 94, 401–419.
Ashton, M., 1993. Advances in Reservoir Geology, vol. 69. Geological Society of London Special Publications.
Besancon, J., Sanlaville, P., 1981. Apercu geomorpholgique sur la vallee de l'Euphrate Syrien. Paleorient 7, 5–18.
Best, J.L., Bristow, C.S., 1993. Braided rivers. Geol. Soc. of London Special Publ. 75.
Best, J., Fielding, C.R., 2019. Describing fluvial systems: linking process to deposits and stratigraphy. Geol. Soc. of London Special Publ. 488, 152–166.
Beydoun, Z., Clarke, M.H., Stonely, R., 1992. Petroleum in the Zagros Basin: A Late Tertiary Foreland Basin Overprinted onto the Outer Edge of a Vast Hydrocarbon-Rich Paleozoic-Mesozoic Passive-Margin Shelf (Chapter 11).
Blum, M., 2019. Organization and reorganization of drainage and sediment routing through time: the Mississippi River System. Geol. Soc. of London Special Publ. 488, 15–45.
Brew, G., Best, J., Barazangi, M., Sawaf, T., 2003. Tectonic evolution of the NE Palmyrides mountain belt, Syria: the Bishri crustal block. J. Geol. Soc. 160, 677–685.
Clark, M., Schoenbohm, L., Royden, L., Whipple, K., Burchfiel, B., Zhang, X., Tang, W., Wang, E., Chen, L., 2004. Surface uplift, tectonics, and erosion of eastern Tibet from large-scale drainage patterns. Tectonics 23.
River to reservoir: geoscience to engineering. In: Corbett, P., Owen, A., Hartley, A., Pla-Pueyo, S., Barreto, D., Hackney, C., Kape, S. (Eds.), Geol. Soc. of London Special Publ. 488.
Demir, T., Westaway, R., Brdigland, D.R., Seyrek, A., 2007. Terrace staircases of the River Euphrates in southeast Turkey, northern Syria and western Iraq: evidence for regional surface uplift. Quat. Sci. Rev. 26, 2844–2863.
Demyanov, V., Arnold, D., Reesink, A., 2019. Can machine learning reveal sedimentological patterns in river deposits? Geol. Soc. of London Special Publ. 488, 221–235.
Dickinson, W.R., 1988. Provenance and Sediment Dispersal in Relation to Paleotectonics and Paleogeography of Sedimentary Basins. In: Kleinspehn, K.L., et al. (Eds.), New Perspectives in Basin Analysis. Springer-Verlag, New York.
Hessami, K., Koyi, H.A., Talbot, C.J., Tabasi, H., Shabanian, E., 2001. Progressive unconformities within an evolving foreland fold–thrust belt, Zagros Mountains. J. Geol. Soc. 158, 969–981.
Hovius, N., Stark, C.P., Tutton, M.A., 1998. Landslide-driven drainage network evolution in a pre-steady-state mountain belt: Finisterre Mountains, Papua New Guinea. Geology 26, 1071–1074.
Jaffey, N., Robertson, A.H.F., 2005. Non-marine sedimentation associated with oligocene-recent exhumation and uplift of the central Taurus mountains, S Turkey. Sediment. Geol. 173, 53–89.
Jolivet, L., Faccenna, C., 2000. Mediterranean extension and the africa-eurasia collision. Tectonics 19, 1095–1106.
Jolley, S.J., Fishers, Q.J., Ainsworth, R.B., Vrolijk, P.J., Delisle, S., 2010. Reservoir Compartmentalisation, vol. 347. Geological Society of London Special Publications.
Leturmy, P., Robin, C., 2010. Tectonic and stratigraphic evolution of Zagros and makran during the mesozoic-cenozoic: introduction. Geol. Soc. of London Special Publ. 330, 1–4.
Litak, R.K., Barazangi, M., Beauchamp, W., Seber, D., Brew, G., Sawaf, T., Al-Youssef, W., 1997. Mesozoic-Cenozoic evolution of the intraplate Euphrates fault system, Syria: implications for regional tectonics. J. Geol. Soc. 154, 653–666.
Marriot, S.B., Alexander, J., 1999. Floodplains: interdisciplinary approaches. Geol. Soc. of London Special Publ. 163.
Martinius, A., Howell, J.A., Good, T.R., 2014. Sediment-body geometry and heterogeneity. Geol. Soc. Spec. Publ. 387.
McQuarrie, N., Van Hinsbergen, D.J., 2013. Retrodeforming the Arabia-Eurasia collision zone: age of collision versus magnitude of continental subduction. Geology 41, 315–318.
Miall, A.D., 1985. Architectural element analysis: a new method of facies analysis applied to fluvial deposits. Earth Sci. Rev. 22, 261–308.
Miall, A.D., 1996. The geology of fluvial deposits. In: Sedimentary Facies, Basin Analysis, and Petroleum Geology. Springer, Berlin.
Miall, A.D., 2006. Case studies of oil and gas fields in fluvial reservoirs. In: The Geology of Fluvial Deposits. Springer, Berlin, Heidelberg.
Miall, A.D., 2010. Fluvial Depositional Systems. Springer, Switzerland.
Nicholson, U., Carter, A., Robinson, P., Macdonald, D.I., 2019. Eocene–Recent drainage evolution of the Colorado River and its precursor: an integrated provenance perspective from SW California.Geological. Society of London Special Publications 488. https://doi.org/10.1144/SP488-2019-272.
Nicholson, U., Es, B., Clift, P.D., Flecker, R., Macdonald, D.I., 2016. The sedimentary and tectonic evolution of the Amur River and North Sakhalin Basin: new evidence from seismic stratigraphy and Neogene–Recent sediment budgets. Basin Res. 28, 273–297.
Nicholson, U., Poynter, S., Clift, P.D., Macdonald, D.I., 2014. Tying catchment to basin in a giant sediment routing system: a source-to-sink study of the Neogene–Recent Amur River and its delta in the North Sakhalin Basin. Geol. Soc. of London Special Publ. 386, 163–193.
Nuriel, P., Weinberger, R., Kylander-Clark, A.R.C., Hacker, B.R., Craddock, J.P., 2017. The onset of the Dead Sea transform based on calcite age-strain analyses. Geology 45, 587–590.
Owen, A., Nichols, G.J., Hartley, A.J., Weissmann, G.S., Scuderi, L.A., 2015. Quantification of a distributive fluvial system: the salt wash DFS of the morrison formation, SW USA. J. Sediment. Res. 85, 544–561.
Ponikarov, V., 1966. Geological map of the Jarablus (J-37-III) quadrangle, 1:200,000 scale. In: Techno-export, Moscow and Ministry of Industry, Syrian Arab Republic (Damascus).
Ponikarov, V., Kazmin, V.G., Mikhailov, I.A., 1967. The geology of Syria: explanatory notes on the geological map of Syria, scale 1:500,000. In: Techno-export, Moscow and Ministry of Industry, Syrian Arab Republic (Damascus).
Richardson, M., Arthur, M.A., 1988. The Gulf of Suez—northern Red Sea neogene rift: a quantitive basin analysis. Mar. Petrol. Geol. 5, 247–270.
Rogl, F., 1999. Mediterranean and Paratethys. Facts and hypotheses of an Oligocene to Miocene paleogeography (short overview). Geol. Carpathica 50, 339–349.

Rose, J.I., Abu-Amero, K., Gonzalez, A., Cabrera, V.M., Larruga, J., Bailey, G.N., Carter, R., Černy, V., Ridl, J., Nasab, H.V., 2010. New light on human prehistory in the arabo-Persian Gulf oasis. Curr. Anthropol. 51, 000-000.
Sharkov, E.V., Chernyshev, I.V., Devyatkin, E.,V., 1998. New data on the geochronology of Upper Cenozoic plateau basalts from the northeastern periphery of the Red Sea Rift area (Northern Syria). Dokl. Earth Sci. 358, 19–22.
Stow, D.A.V., 2005. Sedimentary Rocks in the Field: A Colour Guide. Manson Publishing, p. 320pp.
Trifonov, V.G., Bachmanov, D., Alagili, O., 2012. Cenozoic tectonics and evolution of the Euphrates valley in Syria. Geological Society of London Special Publications 372, 615–635.
Trifonov, V., Bachmanov, D., Ali, O., Dodonov, A., Ivanova, T., Syasko, A., Kachaev, A., Grib, N., Imaev, V., Ali, M., 2013. Cenozoic tectonics and evolution of the Euphrates valley in Syria. Geol. Soc. of London Special Publ. 372, 615–635.
Trifonov, V.G., Dodonov, A.E., Sharkov, E.V., 2011. New data on the Late Cenozoic basaltic volcanism in Syria, applied to its origin. J. Volcanol. Geoth. Res. 199, 177–192.
Weissmann, G.S., Hartley, A.J., Nichols, G.J., Scuderi, L.A., Olson, M.E., Buehler, H., Banteah, R., 2010. Fluvial form in modern continental sedimentary basins: distributive fluvial systems. Geology 38, 39–42.
Whateley, M.K.G., Pickering, K.T., 1989. Deltas: Sites and Traps Fossil Fuel, vol. 18. Geological Society of London Special Publications.
Wheeler, H.E., Cook, E.F., 1954. Structural and stratigraphic significance of the Snake River capture, Idaho-Oregon. J. Geol. 62, 525–536.
Wood, W.W., Bailey, R.M., Hampton, B.A., Kraemer, T.F., Lu, Z., Clark, D.W., James, R.H., Al Ramadan, K., 2012. Rapid late Pleistocene/Holocene uplift and coastal evolution of the southern Arabian (Persian) Gulf. Quat. Res. 77, 215–220.
Yeste, L.M., Henares, S., McDougall, N., García-García, F., Viseras, C., 2019. Towards the Multi-Scale Characterization of Braided Fluvial Geobodies from Outcrop, Core, Georadar and Well Logs Data, vol. 488. Geological Society of London Special Publications, pp. 73–95.

Professor Dorrik Stow FRSE is Professor and former Director at the Institute of Geo-Energy Engineering, Heriot-Watt University, Scotland. He is also Distinguished Professor at the China University of Geoscience, Wuhan, and a Fellow of the Royal Society, Edinburgh. He is an internationally-renowned field and marine sedimentologist who has worked extensively across the world on modern, ancient and subsurface sedimentary systems, with specialization in the deep oceans. He has authored over 300 research papers and several popular science books.

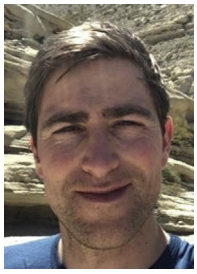

Dr Uisdean Nicholson is an Assistant Professor of Geoscience at Heriot-Watt University. His PhD looked at the interaction of sediment routing systems (particularly large rivers) with active tectonic settings. After his PhD, he spent seven years working for Shell E&P in the Netherlands and Malaysia. Since returning to academia in 2016, his research has been focussed on deepwater sediment routing, using seismic and sedimentological data to understand the evolution of ocean gateways, major current systems, sediment gravity flows and marine geohazards.

Dr Andy Gardiner has an MA in Geology from Cambridge University and a PhD in Fluvio-deltaic Sedimentology from Leeds University. He taught undergraduate geology for seven years, before joining Robertson Research, a UK petroleum consultancy. During thirteen years there, Andy undertook a wide range of exploration and development projects, including geological fieldwork, in the UK, Europe, Africa and Asia. In 1997, Andy joined Heriot-Watt University, where he teaches Reservoir Sedimentology and undertakes research into the use of outcrop analogues in reservoir modelling.

Dr Mahmoud Jaweesh is a hydrogeologist working with the Water Resources Team in Affinity Water, Birmingham, UK. Mahmoud completed his PhD from the School of Geography, University of Birmingham, and then worked as a consultant hydrogeologist at ESI and also was part of the hydrogeology team at Severn Trent Water. The main areas of research are hydrochemistry, surface/groundwater interactions and sustainable abstractions.

Dr Samantha Kearsey carried out research in fluvial sedimentology for her PhD at Plymouth University, UK. She then worked for a period as Teaching Fellow at Heriot-Watt University, Edinburgh, and is now lecturer at Glasgow International College, Scotland.

Mr Dominic Tatum is Research Assistant at the Institute of Geo-Energy Engineering, Heriot Watt University. He has particular research interests in the utilisation of Ground Penetrating Radar for examination of sedimentary rock systems outcropping in the field.

Professor Amer Ghabra was formerly Head of the Department of geology, Damascus University; Head of the Department of Geology and Petroleum Exploration Engineering, and Dean of Faculty of Petroleum Engineering, Syrian Private University, Damascus, Syria, Committeeman of the Mineral Resources Committee, Ministry of Petroleum and Mineral Resources, Syria.He is currently a Head of Petroleum Engineering Department at Al-Amarah University College in Iraq.